

The UNIVERSITY of MICHIGAN

High Energy Physics

500 East University
Ann Arbor, Michigan 48109-1120
Telex: 4320815 UOFM UI
Phone Number: (313) 764-4443

FERMILAB-Proposal-0797

The Harrison M. Randall
Laboratory of Physics

30 August 1988

Leon Lederman
Director
FERMI NATIONAL ACCELERATOR LABORATORY
Batavia, IL 60510

Dear Leon,

A group of us at Michigan are working to develop high-rate fast gas calorimetry and electronics suitable for a high luminosity SSC experiment; a module should be ready to test in about 10 months. We request the use of a FERMILAB testbeam to prove the concepts and implementation.

A copy of our request for Generic SSC Detector R&D Funds is attached. We have developed fast PWC cells for an electromagnetic calorimeter. We intend to use existing electronics to evaluate its performance. We expect to have an ambitious high tech electronics system ready for test somewhat later, and given success would be looking for a high-rate (10^{**8} - 10^{**9}) beam to challenge the system.

We are seeking a test beam with 50-200 GeV protons or pions, some component of electrons, and some means to tag them such as a Cerenkov counter. We would request support of a PDP 11 MULTI based data logging system with BISON BOX, CAMAC crate, and magnetic tape or data link to the VAX cluster. We need PREP support mostly at the level needed to instrument and run the beam line, but including a powered NIM bin, 2 scaler modules, a CAMAC ADC module, 8 discriminators, 6 logic functions, and a gate module; the older LeCroy technology would be fine.

We would like to work on the test beam 2 to 6 shifts a week spread over at least a six month period; a control time estimate would be about 200 hours. Our calorimeter module will be on a table such that it can be moved or lowered out of the beam quickly and expeditiously. We would like our part of the CAMAC crate (8 slots) and our NIM bins to be exclusively for us.

Questions can be addressed to R. Thun (313-936-0792) or R. Gustafson (313-936-0812) at the University of Michigan; or by Decnet MICH::THUN or MICH::GUSTAFSON. We are available to help set up/implement the beam line.

Regards,

R. G.


Dick Gustafson
Rudi Thun

give a good compromise between operating characteristics and handling ease. With these factors in mind, we have chosen to test PWCs with an interior cell width of 3.17 mm and with a sense wire diameter of 38 μ m.

The choice of proportional counter gas involves a number of considerations. The gas must give a sufficient number of ionization electrons, quench avalanche photons to insure stable operation at reasonable gain, exhibit good "aging" properties and yield high drift velocities for operation at SSC. Regarding this last point, research by others³⁻⁸ has shown that drift velocities above 10 cm/ μ sec can be obtained with gas mixtures containing carbon tetrafluoride (CF₄). This is about a factor of two higher than the drift velocity in common mixtures of argon and CO₂ or hydrocarbons.

There is one additional consideration regarding the choice of proportional counter gases for SSC detectors and especially SSC calorimeters. Hadronic showers in such calorimeters will lead to a large flux of low-energy (~ 1 MeV) neutrons which can interact within and outside the calorimeter. Elastic scattering of these neutrons with the protons of any hydrogen component of the PWC gas can result in signals equivalent to those from several hundred minimum-ionizing particles. Such large signals can cause cross-talk problems in tracking chambers or give erroneous energy measurements in calorimeters. For this reason it may be important to minimize or avoid the use of hydrogen in the gas or construction materials of SSC wire chambers.

A gas mixture which minimizes the hydrocarbon content and which has shown good operating characteristics is "HRS gas" consisting by volume of 89% argon, 10% carbon dioxide, and 1% methane.⁹ The small amount of methane helps to absorb avalanche photons at wavelengths around 1200 angstrom where carbon dioxide is relatively transparent. Because of its minimal hydrogen content, HRS gas should be rather immune to low-energy neutrons while also being safe to handle in terms of fire hazard.

In this note we report results from tests of small proportional wire tubes operating with mixtures of CF₄ and HRS gas.¹⁰ The CF₄ is a non-flammable, non-toxic gas which increases the drift velocities markedly. The motivation for these tests is the establishment of parameters for the design of possible SSC prototype wire chambers.

2. EXPERIMENTAL SET-UP

The test wire chamber consists of eight identical square brass tubes arranged in a plane as shown in fig. 1. The length of these tubes is 74.6 mm, the outer width is 3.97 mm, and their wall thickness is 0.40 mm. The maximum drift distance for ionization electrons from perpendicularly incident tracks is therefore 1.59 mm. Each tube contains a 38 μ m diameter gold-plated tungsten wire which is held and centered by a small brass tube inserted into a G-10 fiberglass plug at each end of the chamber tube. Small holes are drilled into the body of each of the eight proportional tubes for gas inlet and outlet and for allowing exposure to an ⁵⁵Fe X-ray source.

At one end of each tube positive high voltage is transmitted to the sense wire through a 1 M Ω resistor. (The brass body of the chamber is held at ground potential). At the other end signals are taken out via a 100 pF decoupling capacitor. For the purposes of this test all eight tubes were gauged together at both the signal and high voltage ends so that the chamber was operated as a single-channel device.

For measurements of rates and drift times, the signals from the chamber were sent to a LeCroy LD604 amplifier-discriminator chip with an input termination of 100 Ω and a threshold of about 0.4 mV. When measuring pulse height spectra with the ⁵⁵Fe source, the chamber signal was routed directly to a Quantum 8 pulse height analyzer.¹¹ Drift time measurements were made with cosmic rays for which the start times were determined with a scintillator placed directly below the chamber as shown in fig. 1. The time interval between the scintillator and chamber signals was converted to a pulse height using a Camberra Model 2043 time analyzer. The output from this time analyzer was then displayed with the Quantum 8 pulse height analyzer.

HRS gas and CF₄ were mixed from separate bottles using flow meters. Care was taken to insure that the total flow of the mixed gas was the same for all mixtures to avoid possible systematic rate-dependent effects when comparing results from different mixtures. This total flow rate was 0.5 cuft/hour.

3. RESULTS

The proportional wire chamber was tested with four gas mixtures consisting of 100% HRS, 20% CF₄ - 80% HRS, 50% CF₄ - 50% HRS, and 100% CF₄ where the percentages are by volume. The first step in testing the chamber was the determination of operating

voltages for each of these mixtures. Figure 2 shows the coincidence rate from cosmic rays of the scintillator and chamber signals as a function of chamber voltage. Figure 3 shows the singles rate from just the chamber versus the applied voltage. In this figure a sudden rise of the singles rate is observed at 1500 V for 100% HRS, 1875 V for 20% CF₄ - 80% HRS, 2250 V for 50% CF₄ - 50% HRS, and 2725 V for 100% CF₄. At these voltages the chamber signals become very large and regenerative causing multiple firing of the amplifier-discriminator chip. These voltages are close to the point of spontaneous chamber breakdown. Comparison of figures 2 and 3 indicates that the width of the voltage plateau for good efficiency varies from about 75 V with 100% HRS to about 200 V for 100% CF₄.

The relative gain of the chamber was measured by observing the peak from the 5.80 MeV X-ray line of an ⁵⁵Fe source. This is displayed in fig. 4 as a function of chamber voltage. The peak from this source is clearly resolved in all gas mixtures except for 100% CF₄ for which the ⁵⁵Fe gives just a very broad, smeared-out distribution. The ⁵⁵Fe spectra for the other three gas mixtures are shown in fig. 5 at voltages giving similar gain. The resolution clearly worsens with increasing fractions of CF₄, an effect already established in ref. 4.

The drift time distributions from cosmic rays, which illuminate the chamber area uniformly, are shown in fig. 6. The operating voltages indicated in the figure correspond to approximately equal chamber gain for the different gas mixtures. We also recorded drift time distributions at somewhat lower and higher voltages and found the widths of these distributions essentially independent of voltage. The width of the drift time range which encompasses 90% of the chamber signals in each distribution is given to the nearest nsec by:

100% HRS:	32 nsec
20% CF ₄ - 80% HRS:	22 nsec
50% CF ₄ - 50% HRS:	19 nsec
100% CF ₄ :	16 nsec

The factor of two decrease in drift times with increasing CF₄ fraction is consistent with the observations in references 3-8.

We note that for uniform illumination of the chamber as in fig. 6, the height of the

drift time distribution at a particular value of the drift time is proportional to the drift velocity at the corresponding position in the cell. As the fraction of CF₄ is increased, one observes a clear asymmetry in the drift time distribution for short and long drift times. The variation in the corresponding drift velocities is roughly a factor of two when the gas is 100% CF₄. When operating the chamber at 2600 V and atmospheric pressure the ratio of electric field to pressure, E/P, varies from about 4.9 V cm⁻¹ torr⁻¹ at the tube wall to 400 V cm⁻¹ torr⁻¹ at the sense wire surface.

4. CONCLUSION

Motivated by a desire to find proportional chamber parameters suitable for use at the SSC, we have tested 3.17 mm wide proportional tubes with several mixtures of CF₄ and HRS gas (89% argon, 10% CO₂, 1% CH₄). As the fraction of CF₄ is varied from zero to 100%, the maximum drift times decrease from about 32 to 16 nsec corresponding to average drift velocities of 5.0 to 10 cm/μsec, respectively. HRS gas was chosen for admixture since its low hydrogen content insures fire safety and promises relative immunity to large pulses from interactions with low-energy neutrons. The operating voltage increases and the energy resolution worsens with increases in the CF₄ fraction. Good efficiency was obtained with all gas mixtures. The voltage plateau increases as the CF₄ component increases. A final judgment of the suitability for SSC use of PWCs as tested here requires further systematic studies of rate capabilities and of chamber degradation with radiation exposure.

5. ACKNOWLEDGEMENTS

We appreciate the loan of equipment from C. Aketlof and F. Becchetti. We also acknowledge many useful discussions with J. Kadyk who is conducting systematic chamber aging studies for various gas mixtures including those containing CF₄. Finally, we appreciate the invitation by M. Gilchriese to participate in SSC detector studies. These studies helped motivate this work.

REFERENCES

1. Report of the Task Force on Detector R & D for the Superconducting Super Collider, SSC-SR-1021 (1986) published by the SSC Central Design Group.
2. Report of the Task Force on Radiation Effects at the SSC, to be published by the SSC Central Design Group.
3. M.S. Naidu and A.N. Prasad, *J. Phys.* **D5** (1972) 983.
4. L.C. Christophorou et al., *Nucl. Inst. and Meth.* **163** (1979) 141.
5. L.C. Christophorou et al., *Nucl. Inst. and Meth.* **171** (1980) 491.
6. J. Fischer et al., *Nucl. Inst. and Meth.* **A238** (1985) 249.
7. R. Henderson et al., TRIUMF preprint TRI-PP-87-84 (1987).
8. R. Henderson et al., *IEEE Trans. on Nucl. Sci.* **NS-34** (1987) 528.
9. D. Koltick, HRS Internal Memo HRS-197 (1980).
10. The HRS mixture was obtained from Air Products & Chemicals, Inc. and the CF₄ was purchased under the trade name of "Freon-14" (99.9% min. purity) from Matheson Company.
11. Manufactured by Nucleus, Inc.

FIGURES

1. Schematic of the proportional wire chamber (PWC) and scintillator used for cosmic ray triggers.
2. Coincidence rate from cosmic rays of PWC and scintillator signals as a function of PWC voltage.
3. Singles rate of the PWC as a function of voltage.
4. Measurement of relative gain as a function of voltage using the peak from the 5.89 KeV X-rays of an ⁵⁵Fe source.
5. Pulse height spectra from ⁵⁵Fe as measured with the PWC.
6. Drift time distributions from cosmic rays as measured with the PWC for several gas mixtures.

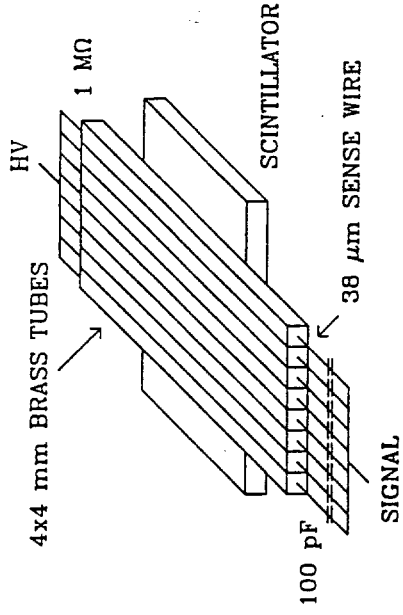


FIG. 1

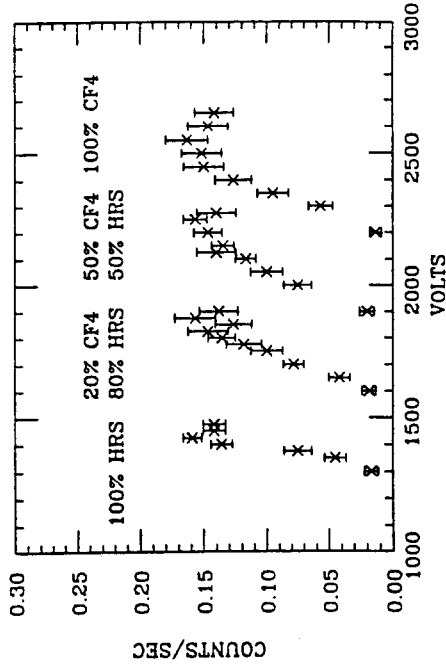


FIG. 2

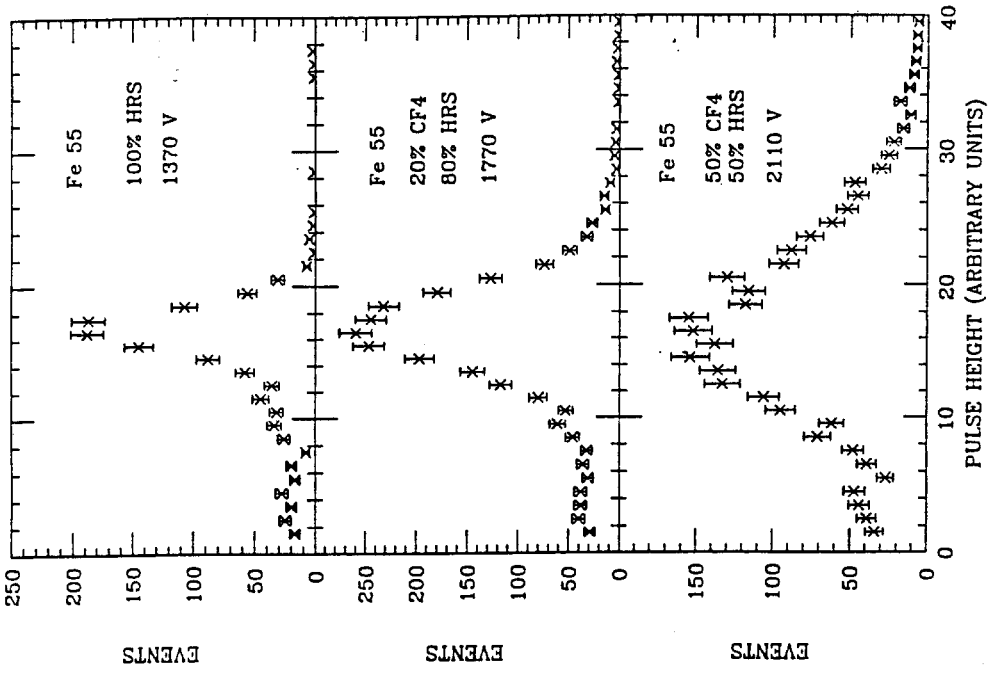


FIG. 5

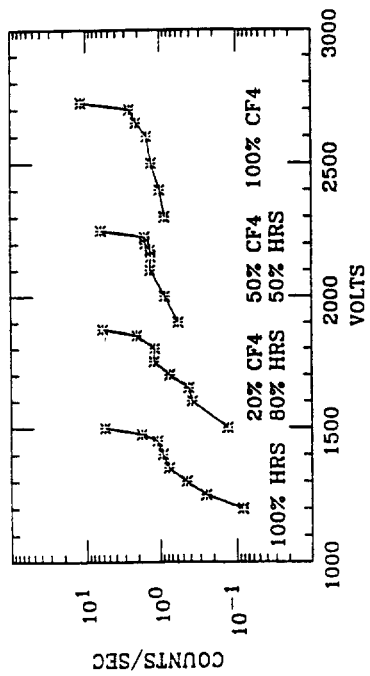


FIG. 3

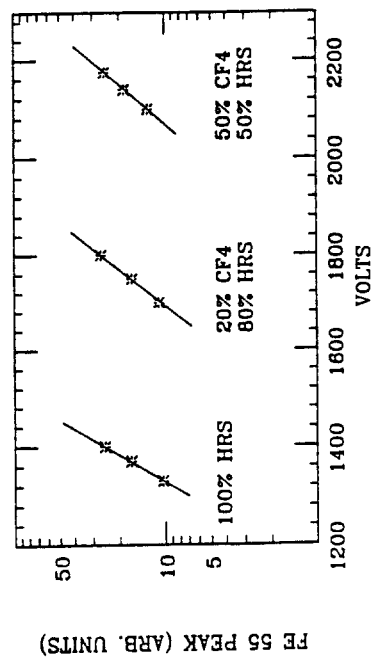


FIG. 4

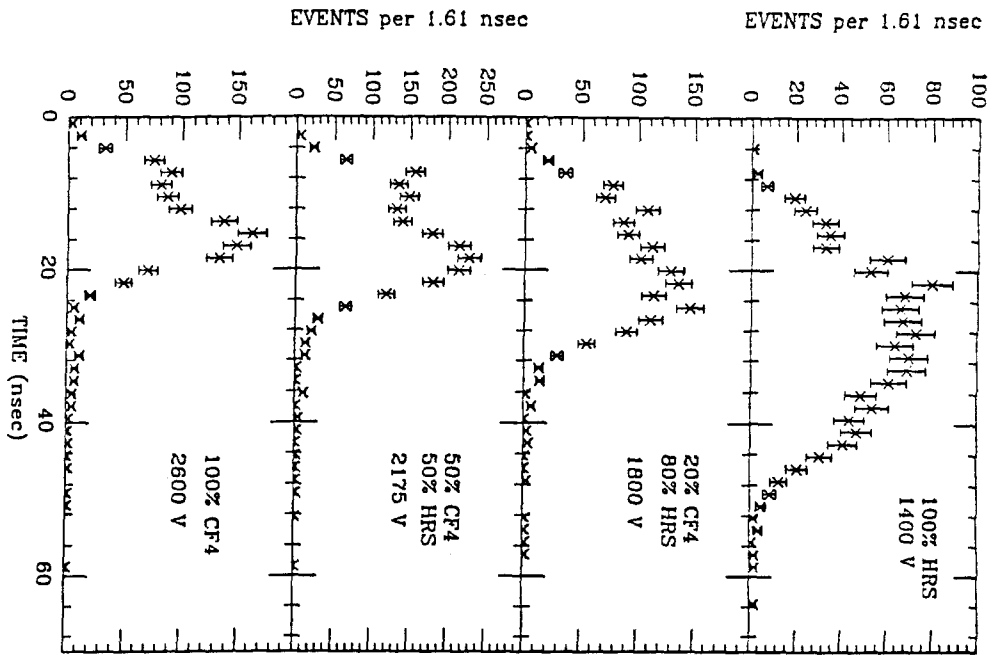


FIG. 6

The UNIVERSITY of MICHIGAN

High Energy Physics

500 East University
Ann Arbor, Michigan 48109-1120
Telex: 4320815 UOFM UI
Phone Number: (313) 764-4443

FERMILAB-Proposal-0797

The Harrison M. Randall
Laboratory of Physics

Leon Lederman
Director
FERMI NATIONAL ACCELERATOR LABORATORY
Batavia, IL 60510

30 August 1988

Dear Leon,

A group of us at Michigan are working to develop high-rate fast gas calorimetry and electronics suitable for a high luminosity SSC experiment; a module should be ready to test in about 10 months. We request the use of a FERMILAB testbeam to prove the concepts and implementation.

A copy of our request for Generic SSC Detector R&D Funds is attached. We have developed fast PWC cells for an electromagnetic calorimeter. We intend to use existing electronics to evaluate its performance. We expect to have an ambitious high tech electronics system ready for test somewhat later, and given success would be looking for a high-rate (10^{**8} - 10^{**9}) beam to challenge the system.

We are seeking a test beam with 50-200 GeV protons or pions, some component of electrons, and some means to tag them such as a Cerenkov counter. We would request support of a PDP 11 MULTI based data logging system with BISON BOX, CAMAC crate, and magnetic tape or data link to the VAX cluster. We need PREP support mostly at the level needed to instrument and run the beam line, but including a powered NIM bin, 2 scaler modules, a CAMAC ADC module, 8 discriminators, 6 logic functions, and a gate module; the older LeCroy technology would be fine.

We would like to work on the test beam 2 to 6 shifts a week spread over at least a six month period; a control time estimate would be about 200 hours. Our calorimeter module will be on a table such that it can be moved or lowered out of the beam quickly and expeditiously. We would like our part of the CAMAC crate (8 slots) and our NIM bins to be exclusively for us.

Questions can be addressed to R. Thun (313-936-0792) or R. Gustafson (313-936-0812) at the University of Michigan; or by Decnet MICH::THUN or MICH::GUSTAFSON. We are available to help set up/implement the beam line.

Regards,

R. G.


Dick Gustafson
Rudi Thun

Proposal to Develop SSC Detectors Based on Small-Diameter, Fast-Drift Proportional Tubes.

R. Ball, J. Chapman, R. Gustafson, G. Mills, B. Roe, R. Thun

*University of Michigan
Ann Arbor, MI 48109*

Abstract

We propose to construct, instrument and test a fine-grained electromagnetic calorimeter based on small-diameter proportional tubes with maximum drift times of about 20 nsec. Construction of the calorimeter and configuration with existing electronics will be completed within one year. Development of specialized, fast, radiation-hard electronics will require somewhat more time. We request \$140,400 for this project of which \$101,250 is to be allocated for the required electronics R&D. We propose to test the calorimeter in a Fermilab test beam.

I. Introduction

One of the great challenges posed by the Superconducting Super Collider (SSC) is the enormous event rate (10^8 Hz). Such a rate produces event pile-up with most of the commonly used detector techniques. For example, typical gas-based drift chambers as well as liquid-based calorimeters involve signal collection times of order several hundred nanoseconds or more. The corresponding electronic gates used in the trigger and data collection will necessarily involve the overlap of tens of events when using such detectors. The problem of extracting the hidden physics jewels in the general debris of hadronic collisions is well known. One would, therefore, like to eliminate any additional problems from event pile-up. It is sometimes remarked that such pile-up only involves the overlay of minimum-bias events with a transverse energy so low as not to corrupt the interesting physics. However, the rate of random coincidences scales directly with the duration of the trigger gates. For example, two randomly coincident jet-jet events will enter the 4-jet sample and it is not obvious how easily such background events are rejected in the off-line analysis.

It is clear that ideally one would like to reduce the jitter in signal-collection times to the order of $1/\text{EVENT RATE} \sim 10$ ns. Shorter times yield little additional advantage since finite detector sizes introduce a jitter of that order just from variations in signal traversal times.

We propose to develop proportional-wire detectors with short ($\lesssim 20$ ns) signal collection times. Specifically, for our first detector we plan to construct a prototype of a fine-sampling electromagnetic calorimeter which could be used for the simultaneous measurements of energy and particle direction. Such a detector might find application in the interior of a large muon-oriented spectrometer. Although we necessarily pick a specific prototype detector, what we will learn will have broad "generic" applicability to any tracking or calorimetric device based on fast proportional tubes.

II. Summary of Research Already Completed at Michigan

Through a "redirection of effort" (made possible in part by the slow turn-on of SLC) we have started a program of research at Michigan to find parameters suitable for SSC proportional chambers. This program has focussed so far on two topics: a search for gasses with high drift velocities and a study of the effects of neutrons on the operation

of proportional chambers. The initial part of this work is documented in the attached preprint which has been accepted for publication in Nucl. Inst. and Methods. The main result of this paper is that maximum drift times as low as 16 ns are achievable with 4 mm wide proportional tubes operating with mixtures of HRS gas (89% Ar - 10% CO₂ - 1% CH₄) and CF₄. We have extended this work to a wide variety of other gas mixtures as shown in Figures 1 thru 4. Particularly promising are Ar - CO₂ mixtures which show drift velocities approaching those of the HRS - CF₄ mixtures.

We have also made a study of the effect of neutrons on proportional tube performance as a function of chamber gas. Our interest here is to understand the so-called "Texas Tower" effect observed in the Fermilab CDF experiment where occasionally very large pulses are observed inside a wire-chamber calorimeter. It is thought that the effect is primarily due to elastic scattering of ~ 1 MeV cascade neutrons with hydrogen protons in the chamber gas and structure. The slow recoil protons are heavily ionizing and can leave a signal equivalent to several hundred minimum-ionizing particles. To test this hypothesis we exposed a chamber to a 925 mCi Am-Be source which yields approximately 2×10^6 neutrons per second with an energy spectrum from 1 to 5 MeV. The neutrons were moderated somewhat by several cm of paraffin. Gamma rays from the $\alpha + Be \rightarrow C^* + n$ reaction were absorbed with 1.3 cm of lead placed between the chamber and source. Preliminary data, displayed in Figures 5 & 6, show a definite increase in the rate of large chamber pulses when increasing the hydrogen content of the gas. Fortunately both CO₂ and CF₄ are quenching gasses with large drift velocities and no free protons.

The members of our group involved in the construction of the L3 hadron calorimeter have also studied the effect of neutrons, and were among the first to demonstrate that neutrons, and specifically the large recoil proton pulses, were a major part of the uranium calorimeter "compensation." By using gasses with varying amounts of hydrogen in a test beam at CERN it was possible to vary the π/e ratio from about 0.8 to well above 1 for a test uranium - PWC calorimeter.

III. Prototype Detector

The original motivation for the work discussed in Section II came from a consideration of how to instrument the absorber of a muon spectrometer (see Figure 7) to allow the measurement of isolated electrons and of hadronic energy flow. The requirement of fast,

radiation-hard detectors led to the idea of using small proportional tubes with fast gasses and operated at low gain (10^3 - 10^4). A geometry for implementing a calorimeter based on such tubes is sketched in Figure 8. The calorimeter is built up with planes containing alternating tubes and radiators placed transversely to the beams in a coaxial cylindrical stack. The planes are oriented in varying directions to create a fairly homogeneous calorimeter with a response that is essentially independent of the longitudinal position of the proton-proton collision point and independent of particle angle. Each plane yields a spatial coordinate of the shower so that the calorimeter can be used for both the track and energy measurements of showering particles. By running at a suitably low gain the calorimeter can be made insensitive to minimum-ionizing tracks and low-energy photons while being obviously sensitive to showering particles with "interesting" energies ($E \gtrsim 100$ GeV).

We propose to build a prototype calorimeter suitable for test beam use. As shown in Figures 9 and 10 the prototype consists of a stack of square planes oriented in a repeating series of $0^\circ - 45^\circ - 90^\circ - 135^\circ$ sets. Each plane consists of alternating tubes and radiators with a width of about 4 mm. We have not yet decided between lead and tungsten as the radiator material. For lead a radiation length is 0.56 cm and the Moliere radius is 1.6 cm while for tungsten the values are 0.35 cm and 0.92 cm respectively. Tungsten yields more compact showers but is therefore also more sensitive to the granularity of the calorimeter. The prototype calorimeter will be made about 30 radiation lengths deep and will contain of order 600 proportional tubes.

IV. Existing Electronics

We have available to us at Michigan several systems of charge digitizing electronics for chambers. These are available immediately; we have the operational experience to believe they can be set up expeditiously and used with no surprises.

The first system, designed and built by Ball, Gustafson, Longo, and Roberts, is composed of 8-channel cards, a controller-processor powering, reading and digitizing up to 255 channels, and a CAMAC interface reading up to 256 controllers. The card channel density is one per inch on a 3" x 8" card. Digitization is 12 bit (4096 with a sensitivity of about 2 femtocoulombs per count; pedestals are at about channel 100). There is a high impedance version with noise sigma of about 1 channel (2 femtocoulombs). A low impedance (25 ohm)

version for possible charge division has a noise of 3 channels (12 femtocoulombs). A test charge injection calibration scheme is included. A gate is applied to the controller about 0.7 microseconds after the event passage; the effective gate width is about 2 microseconds. Digitization requires 25 microseconds per channel with controller operating in parallel. A sparse scan system is included. Readout of the controllers proceeds at CAMAC speeds.

8500 channels of the high impedance system were used in FNAL E613 at a cost of about \$7/channel. A current inventory of available units shows at least 1000 channels with 7 controllers, and a CAMAC interface.

The low impedance system, designed and built by R. Gustafson, is also available. This consists of 12" boards, 3/8" per channel, 32 channels per board, with 25 ohm input impedance and, a gate time of 120 nanoseconds. Forty-two working boards exist. There are onboard delay lines which delay and clip the integrated charges; the gate signal is applied 450 nanoseconds after the input charge. The charge sensitivity is 4 femtocoulombs per channel with a noise sigma of 3 channels. The readout, control, and calibration systems are the same as for the slower system and the components can be mixed. This system ran in FNAL E711.

These systems require a conventional CAMAC crate based data acquisition system. A PDP 11 based MULTI system with BISON box and magnetic tape logging would be adequate.

A third system consists of 1000 channels of conventional LeCroy FASTBUS ADCs which are presently available. Characteristics are 50 femtocoulomb/count, 50 ns minimum gate, 15 bits, 96 channel per board, 300 microsecond conversion time, and a readout rate of 7 megaword/sec. A computer based data acquisition system with a fastbus interface would be required. Alternately the system could be read out through CAMAC.

V. New, Fast Electronics

The existing electronics, though acceptable for detector studies, are not usable in a high rate environment. For the SSC, one would like to implement fast electronics in high density, radiation hardened integrated circuits that can be manufactured at low item costs. We propose to pursue this goal with the help of the newly established University of Michigan integrated circuit laboratory associated with the Engineering School. We have acquired two CAD stations that are network linked to the Engineering School and execute

the same design and simulation software used there. We also have a staff engineer, Maher Siraj, who is familiar with the software and procedures of the Engineering School. He will undertake the electronics development.

The starting point for this development will be the fast pulse designs developed by Radeka¹. These circuits provide clipped and shaped pulses of less than 10ns. The fabrication of these bipolar circuits using indium contacts to silicon wafer based interconnects looks promising for compactness and flexibility. The resistance of the complete package to neutrons and ionizing radiation will be evaluated with the help of the University of Michigan Phoenix reactor where fluxes of neutrons from modest to very intense exposures are available. Bipolar circuits are noted to be subject to permanent damage from neutrons.

A promising alternate approach is to use the fastest available MESFETs. These circuits are less sensitive to neutron damage and can be constructed with higher densities. They are known to suffer temporary disturbances in their insulating layers due to ionizing radiation but this sensitivity has been reduced in recent years. If circuits of sufficient speed can be designed and simulated using this technology, prototypes will be constructed and their performance and radiation resistance to ionizing radiation tested.

Attention will be directed to providing for local fast signal processing in the design of the front-end electronics. This will hopefully provide entry for the development of hierarchical trigger processing in the future should the proposed detector and electronics scheme prove effective and sufficiently radiation resistant. Test readout of the fast electronics will utilize the FASTBUS ADCs mentioned above.

VI. Test Beam

We are requesting the use of a FERMILAB test beam for testing the calorimeter module. We hope to determine basic operating characteristics about one year from now, and then to move into a high rate test behind some running experiment. We append a copy of the test beam proposal letter to FNAL. We expect to adapt our existing electronics to test the calorimeter in a modest rate environment with a 50-200 GeV beam containing hadrons and electrons. The high rate tests will use the new electronics to cope with the pile up and rate problems, and the realities of high chamber currents.

VII. Radiation Test Facility

A major type of radiation for the detectors environment is expected to be neutrons in the neighborhood of 1 MeV. For a detector situated at 2 meters from the interaction of the neutron fluence is expected to be of the order of $2 \times 10^{12}/\text{cm}^2/\text{yr}$.

The University of Michigan Phoenix Nuclear Reactor can provide a test facility for us to expose PWCs and/or electronics, powered or unpowered. Packages of 2" diameter and up to 20" long can be exposed to fluences of between 3×10^8 and 2×10^{12} neutrons (> 1 MeV)/ cm^2/sec . (The package should be somewhat shorter to keep the dosage reasonably uniform over the package.) The staff of the reactor have expressed their willingness to cooperate with us in this effort.

VIII. Time Scales

Our intention is to have the prototype calorimeter ready by the summer of 1989. Existing electronics will be collected and reconfigured for this prototype on the same time scale. Measurements in a test beam would be conducted during the second half of 1989, the exact time depending on the availability of a suitable test beam.

The time scale for the development of new, fast electronics is more difficult to predict because of the more fundamental R & D effort required for design and fabrication. The goal would be to have such electronics ready by the end of 1989.

IX. Budget

The budget for this project is divided into four major areas:

- 1.) Fabrication of prototype calorimeter
 - a.) Materiel \$ 4,000.00
 - b.) Machining and assembly \$ 8,000.00
- 2.) Reconfiguration of existing electronics (including new cables and connectors) \$ 9,000.00
- 3.) Travel to test beam and operational funds (gas, plumbing, etc.) \$ 6,000.00
- 4.) Reactor access fee \$ 2,000.00
- 5.) R & D and fabrication of new, fast electronics

a.) Prototype mask and IC supplies	\$ 30,000.00
b.) Electronics Shop charges	\$ 20,000.00
c.) IC Laboratory fees	\$ 15,000.00
d.) Computer design and simulation costs	<u>\$ 10,000.00</u>
Total direct cost	\$104,000.00
35% MTDC (indirect costs)	<u>\$ 36,400.00</u>
	TOTAL \$140,400.00

X. Manpower and Responsibilities

The responsibilities for this project are divided as follows:

- 1.) Design and fabrication of calorimeter - R. Thun
- 2.) Reconfiguration of existing electronics - R. Gustafson, B. Roe, R. Ball
- 3.) Test beam set-up - R. Gustafson
- 4.) New electronics - J. Chapman
- 5.) Test beam measurements - all

XI. References

- 1.) J. Fischer, et al., NIM A238 (1985) 249

Figures

- 1.) Drift-time distributions from the traversal of cosmic rays through 4 mm wide proportional tubes. Distributions are for various Ar- CO₂ mixtures.
- 2.) Fe⁵⁵ spectra for various Ar-CO₂ mixtures.
- 3.) Drift-time distributions for various Ar-CO₂-CF₄ mixture in the 4 mm proportional tubes.
- 4.) Drift time distributions for pure quenching gasses in the 4 mm proportional tubes.
- 5.) Pulse height spectra from a drift chamber exposed to an Am-Be source as a function of lead absorber between chamber and source. The lead absorbs gamma rays which yield counts at low pulse height. The lead has no effect on counts with large pulse height which are generated by neutron-proton elastic scattering.

- 6.) Pulse height spectra from a drift chamber exposed to an Am-Be source as a function of various gas mixtures. For each mixture, the voltage was chosen to give equal gain as determined with an Fe^{55} source. As the hydrogen content of the gas is increased, a significant increase of counts with large pulse height is observed. This presumably originates from neutron-proton elastic scattering.
- 7.) Possible detector lay-out for a muon spectrometer. A major challenge is the instrumentation of the absorber to measure electron and hadronic jet energies.
- 8.) A possible geometry for an electromagnetic calorimeter inside the absorber of the muon spectrometer.
- 9.) Prototype electromagnetic calorimeter. Each layer consists of alternating proportional tubes and radiator (either tungsten or lead).
- 10.) Orientation of layers in the prototype calorimeter. The sequence is a repeating set of $0^\circ - 45^\circ - 90^\circ - 135^\circ$ orientations.

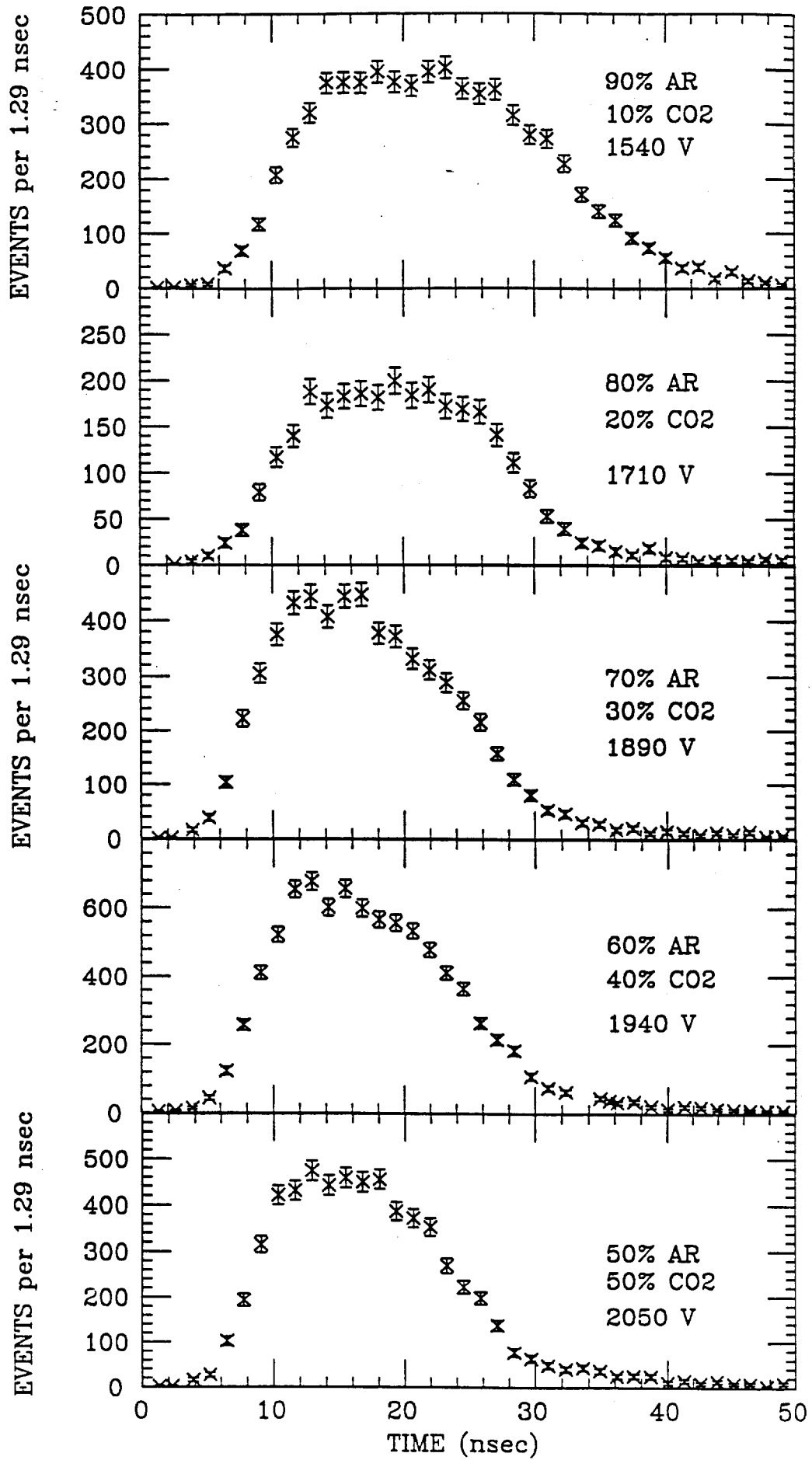


FIG. 1

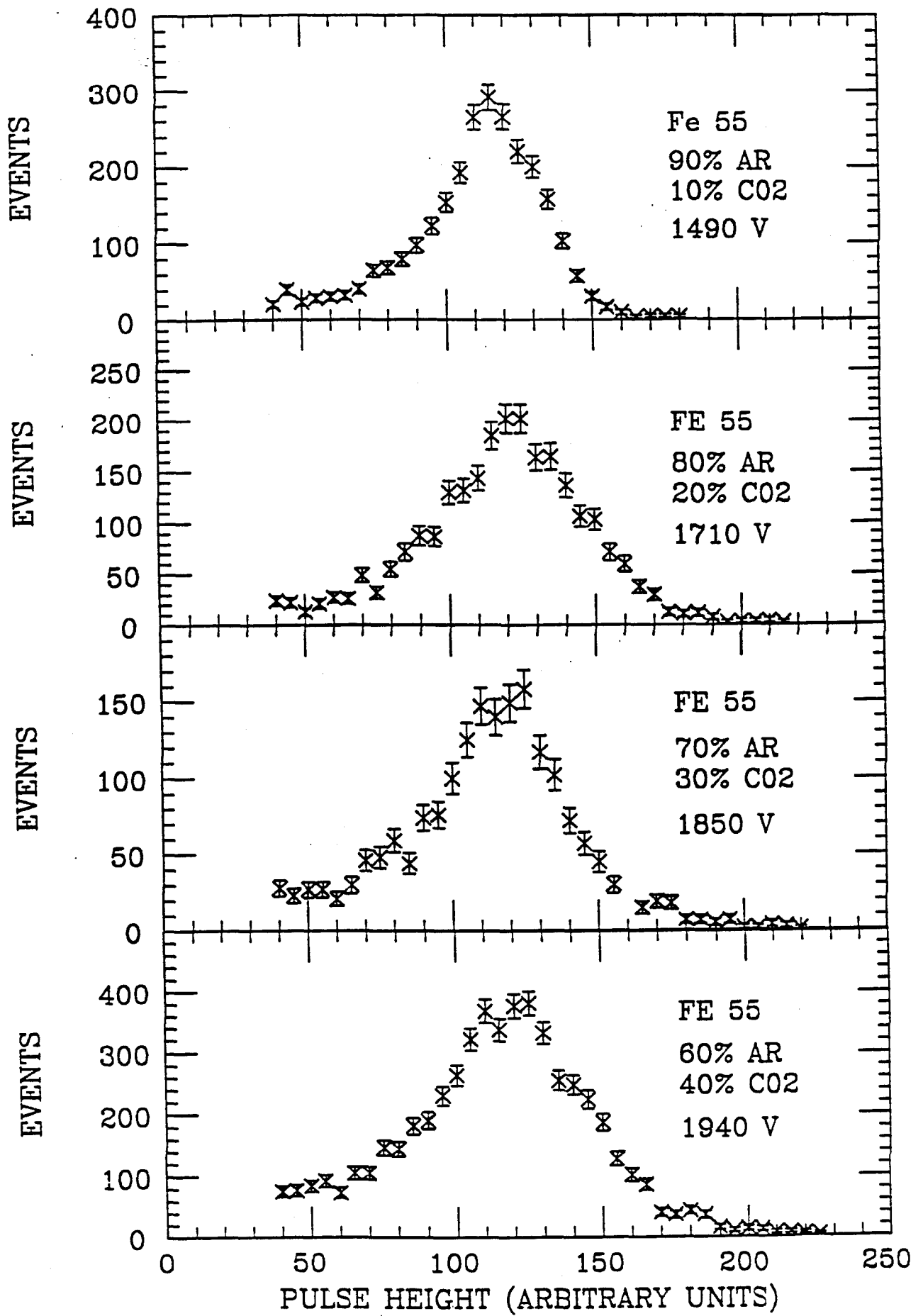


FIG. 2

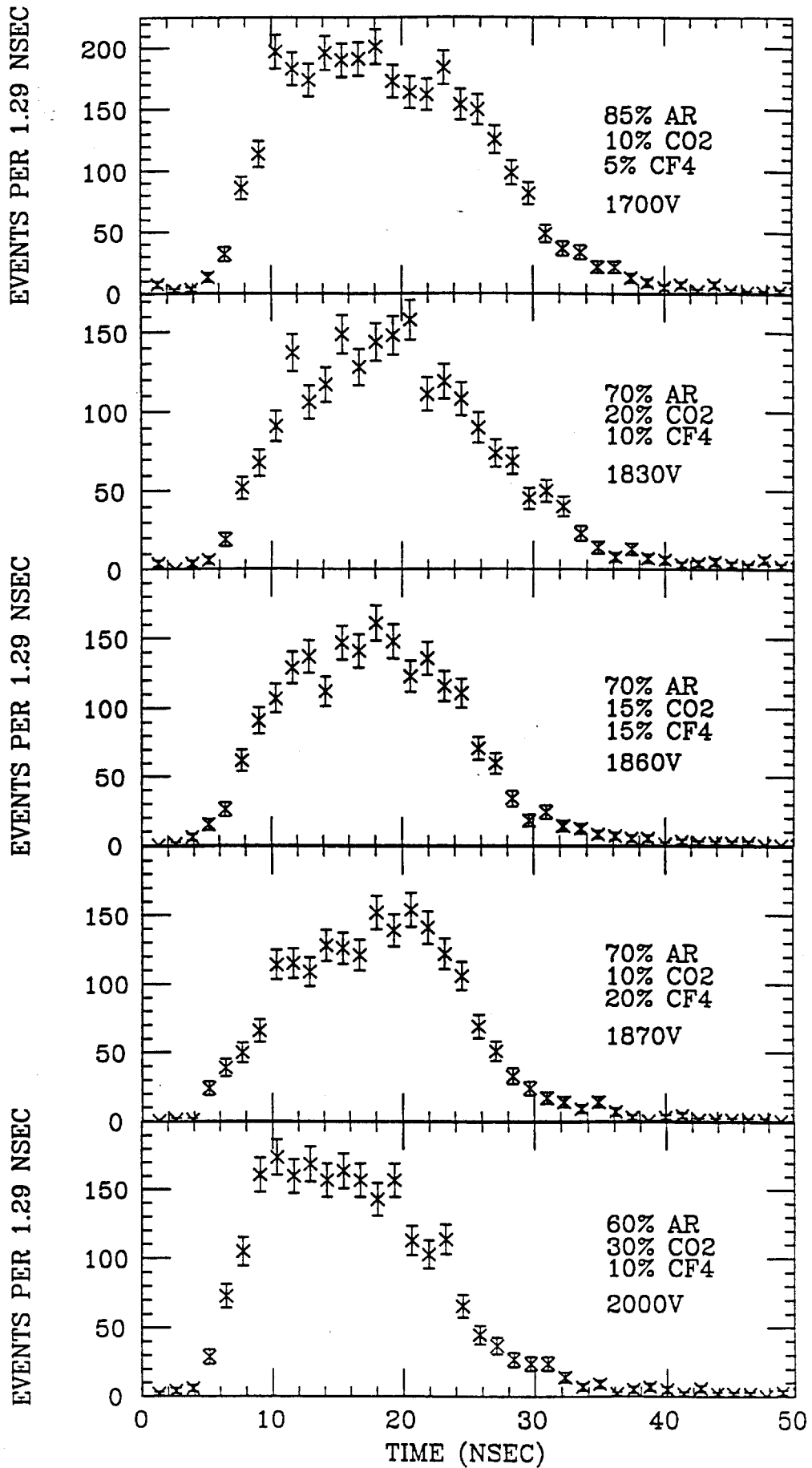


FIG. 3

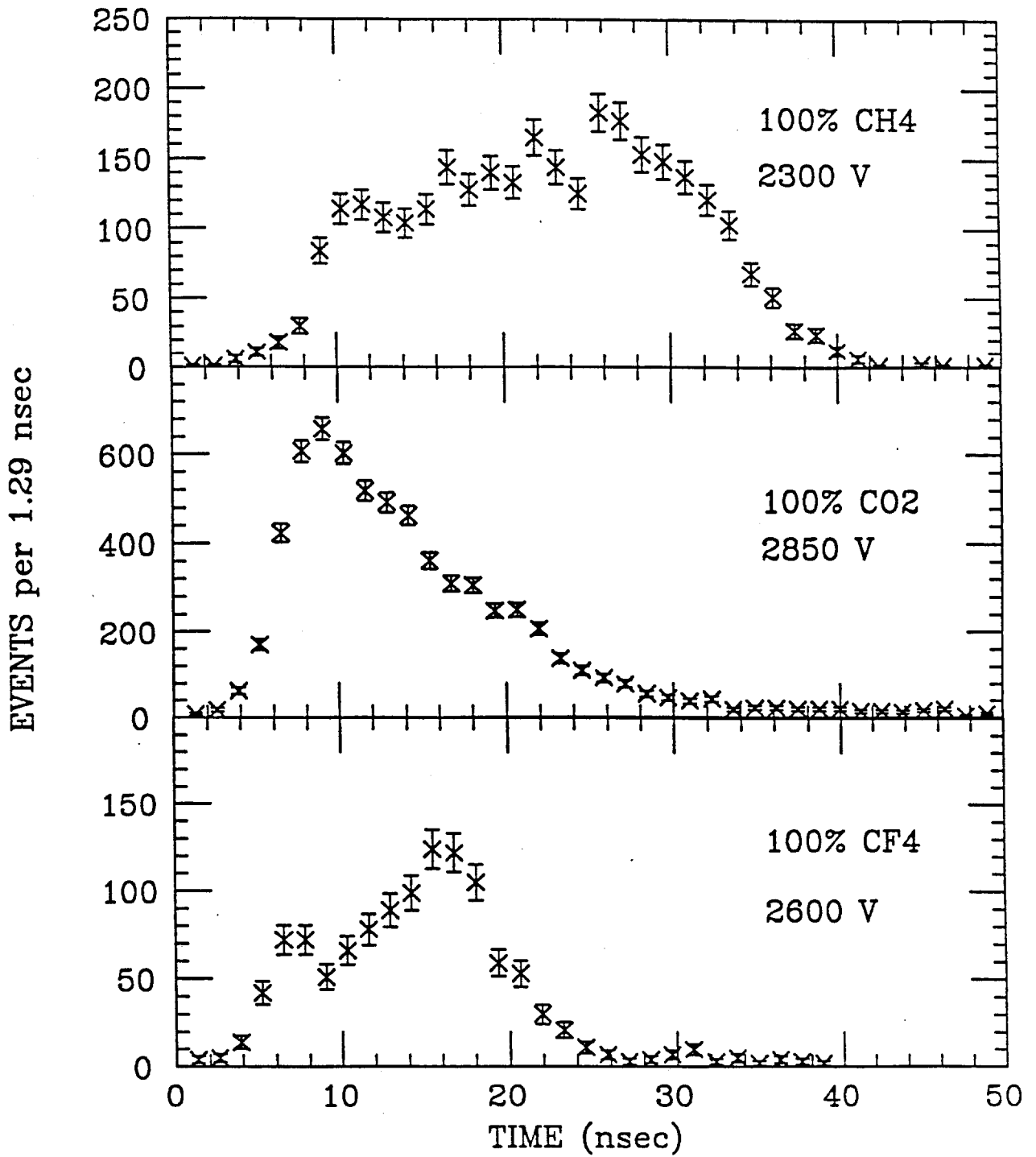


FIG. 4

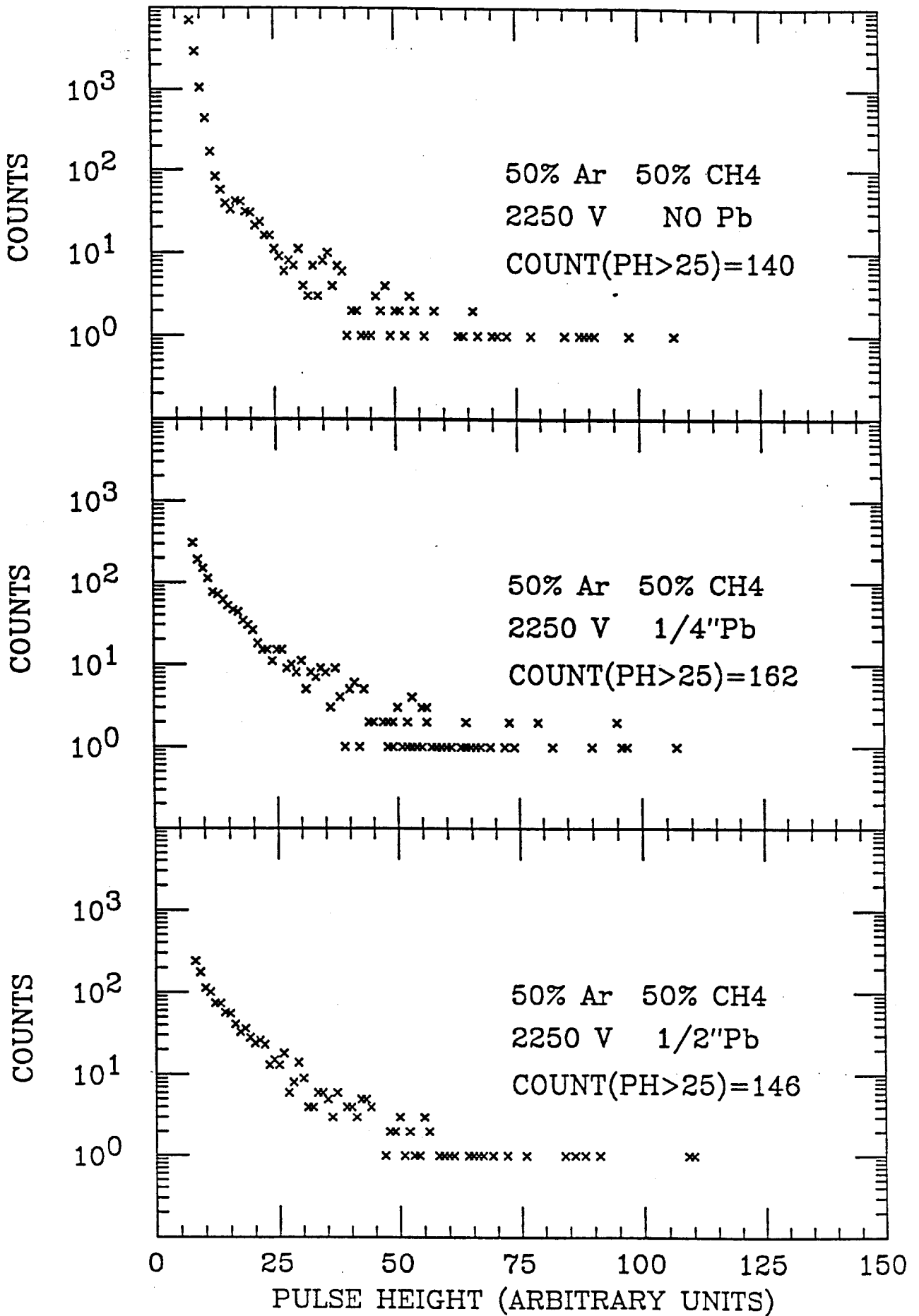


FIG. 5

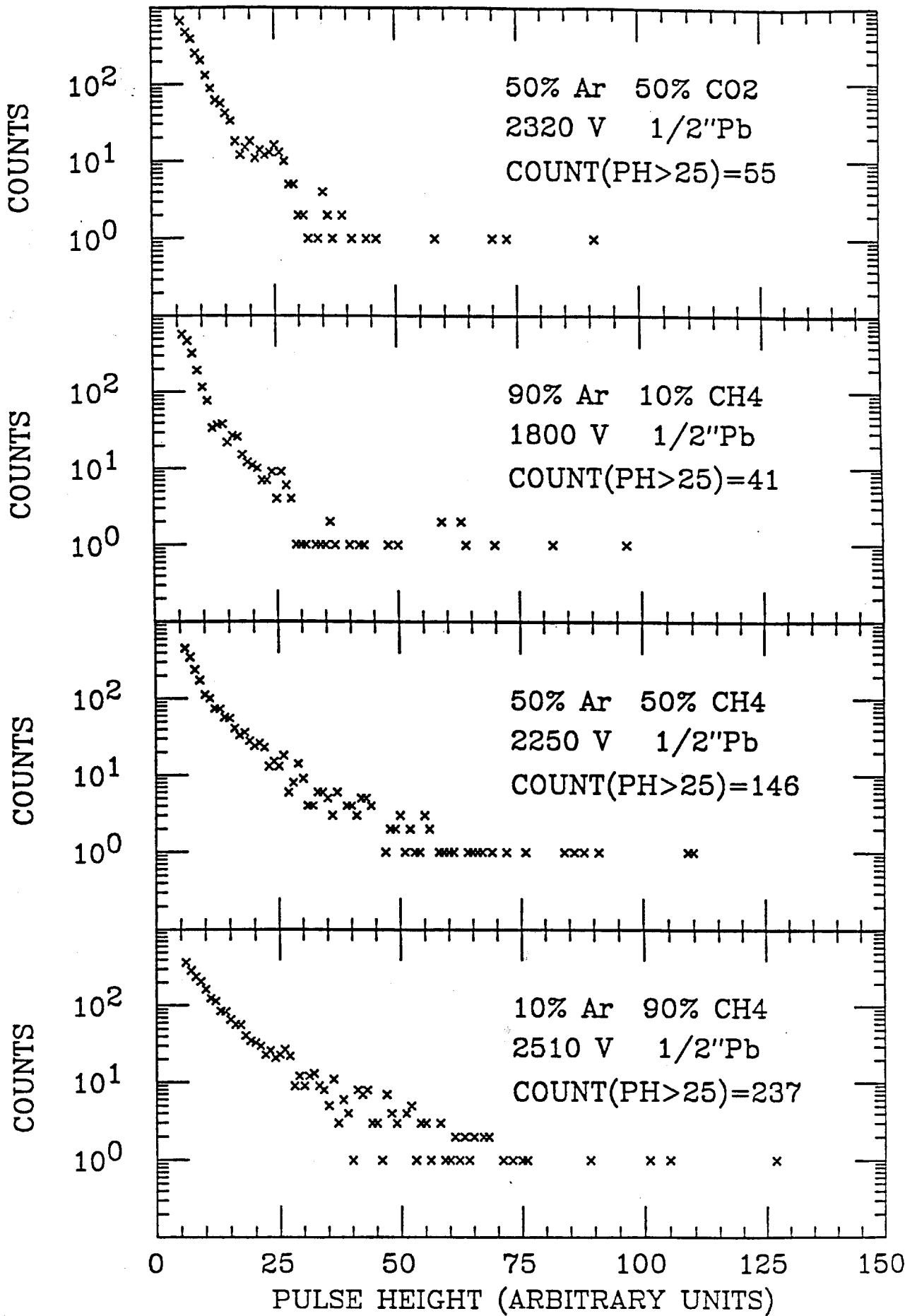


FIG. 6

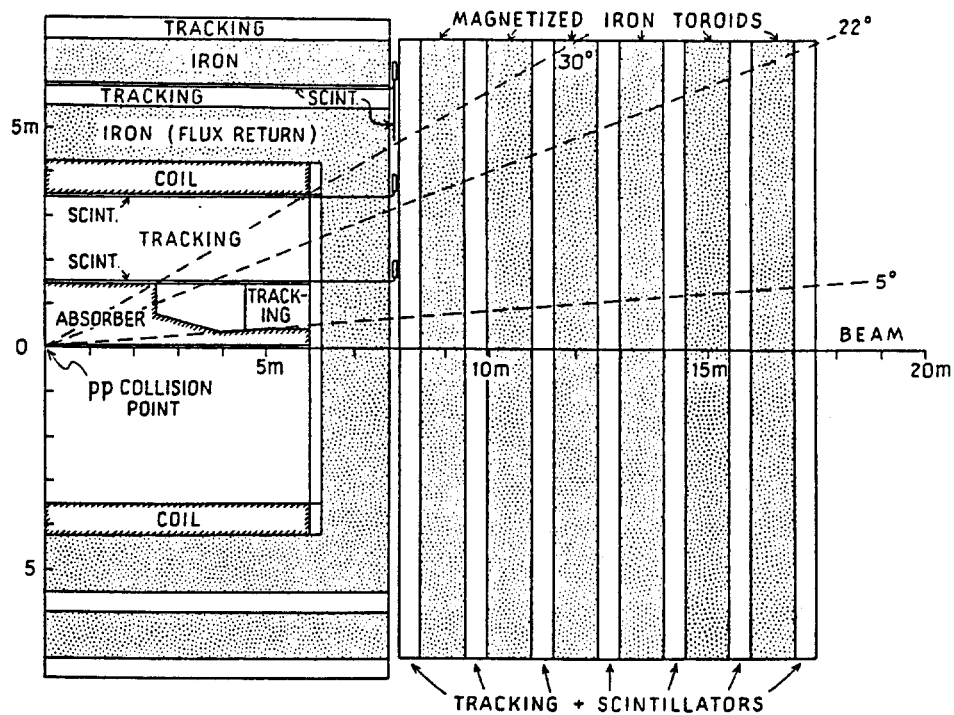


FIG. 7 Side view of muon detector. The detector is symmetric about the collision point and only the right half is shown.

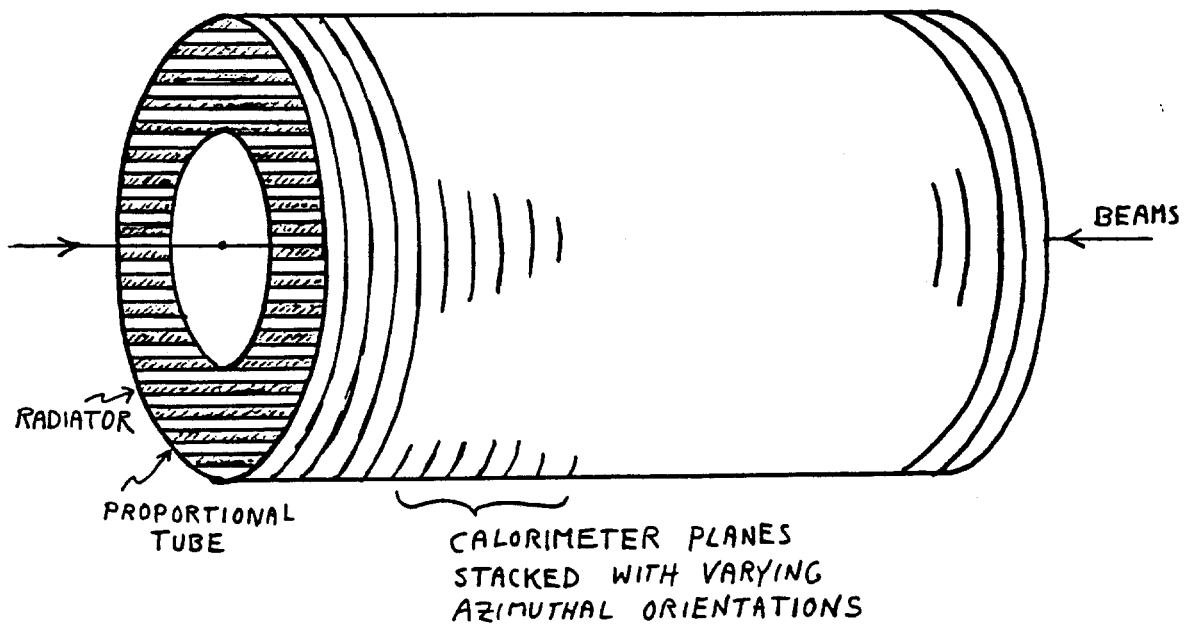


FIG. 8

FIG. 9

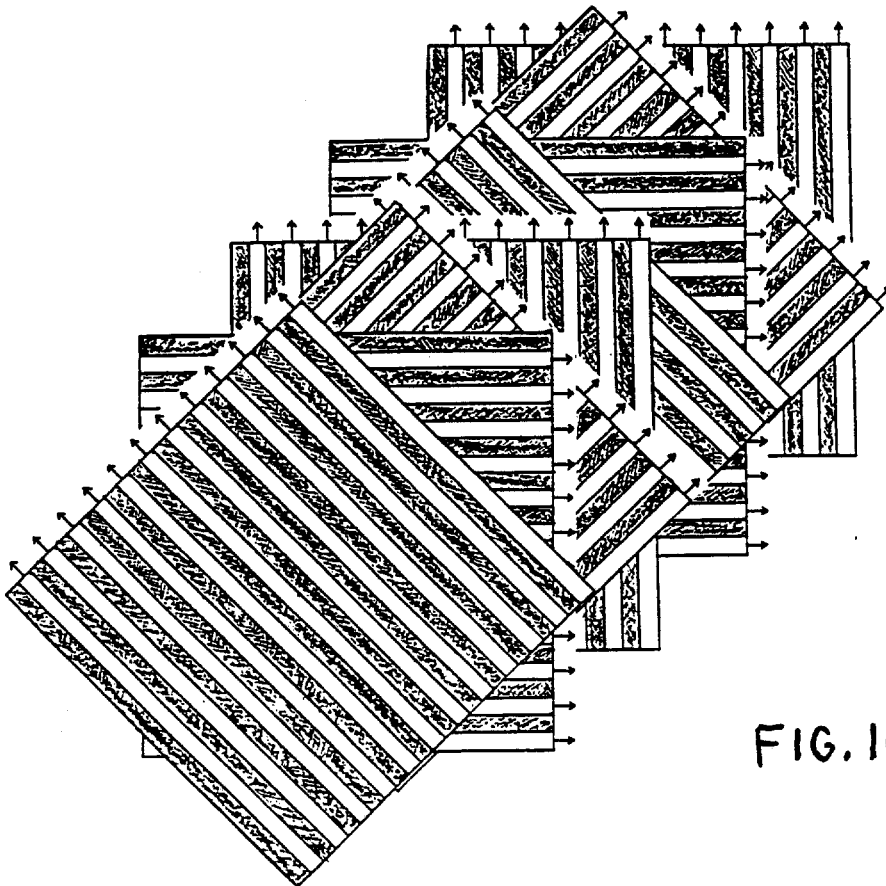
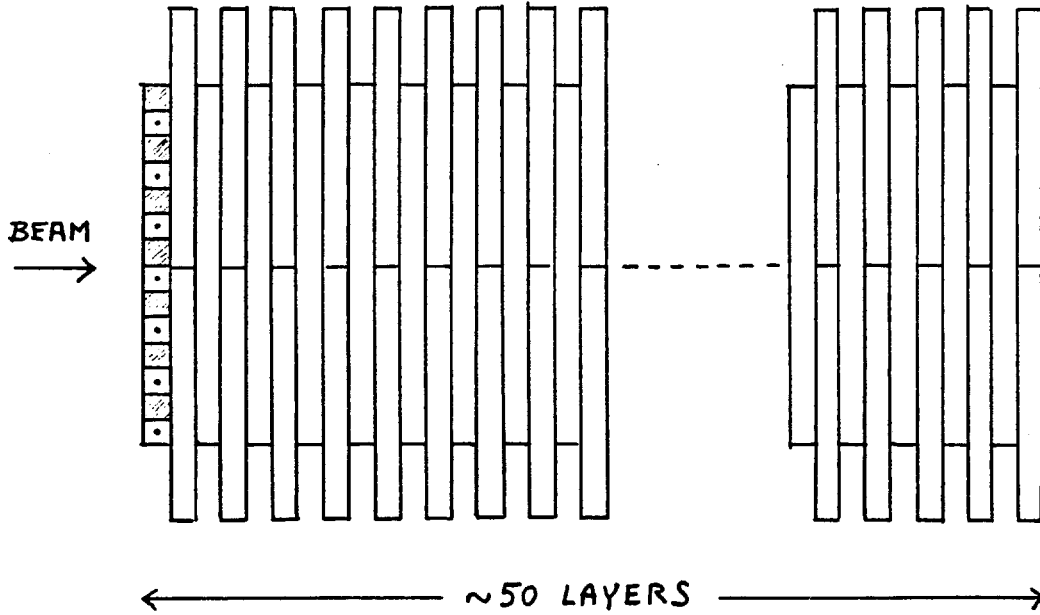


FIG. 10

Tests of Small Proportional Tubes with CF_4 - HRS Gas Mixtures

R. THUN

University of Michigan, Ann Arbor, Michigan 48109

Abstract

We have investigated the operating characteristics and drift times of small proportional tubes (active width = 3.17 mm) containing mixtures of CF_4 and HRS gas (80% Ar, 10% CO_2 , 1% CH_4). As the fraction of CF_4 is varied from zero to 100%, maximum drift times decrease from about 32 nsec to 16 nsec. The operating voltage increases and the energy resolution worsens significantly with increases in the CF_4 component.

(submitted to Nuclear Instruments and Methods)

1. INTRODUCTION

The proposed Superconducting Super Collider (SSC) presents a very challenging environment to the designers of experiments.¹ At the expected luminosity of $10^{33} \text{ cm}^{-2} \text{ sec}^{-1}$ the inelastic collision rate is about 10^8 per second with each event generating on average about 100 secondary particles. Three basic problems must be addressed when planning for SSC experiments: rates, radiation damage, and the implementation of suitable triggers. We believe it will be exceedingly important to reduce the spread in signal arrival times within an event down to a level where event pile-up is a manageable problem. Since the average time between events is 10 nsec, it is desirable that the time smearing of signals approach this value.

Proportional wire chamber (PWC) technology has been an essential component of many high energy physics experiments. Indeed, nearly all tracking of charged particles has been done with this versatile detection method. PWCs have also found major application in both electromagnetic and hadronic calorimetry. Such calorimetry will play a central role in most SSC experiments. Wire chambers have a number of properties which make them attractive for SSC detectors. Their application to apparatus with large areas or volumes is comparatively inexpensive and their construction is generally straight-forward. Unlike scintillating or semiconducting materials, wire chambers are rather immune to radiation damage when not powered. This is a potential advantage during SSC machine development and beam manipulations. However, to be suitable as SSC detectors, wire chambers must satisfy certain radiation or "aging" requirements² and they must allow fast signal collection times as indicated above. These requirements lead naturally to the consideration of chambers with small cell diameters and the use of gases with high drift velocities.

In our judgement ease of construction is an important factor for detector systems that may contain tens of thousands of proportional cells. This effectively places a lower limit on the cell diameter of about 3 to 4 mm. This follows from the observation that large chamber systems are best operated at atmospheric pressure where the typical number of ionization electrons per mm of track length is about ten. Moreover, the mechanical problems of handling cells much smaller than 3 mm are formidable. Mechanical considerations also lead one to a choice of sense wire diameters that are not too small. Operating voltages increase only slowly with diameter whereas the mechanical strength varies as the square of that dimension. We have found from experience that sense wires with a diameter of 38 μm

FERMILAB-Proposal-0797

wave propagation in z direction only. Then one may use a linearized form of the wave equation (Raffelt and Stodolsky 1988), $i\partial_z\psi = n\omega\psi$, where n is the refractive index for this wave. For relativistic particles with mass m it is given as $n = 1 - m^2/2\omega^2$ so that the momentum of the particle is $|\mathbf{k}| = \omega - m^2/2\omega$. We are concerned with a situation where ψ is a two-component vector and n is a 2×2 matrix with generally complex entries.

If one considers the propagation of axions and photons in the presence of a (nearly homogeneous) magnetic field \mathbf{B} , one finds from very general arguments (Raffelt and Stodolsky 1988) that only the photon component with polarization parallel to the magnetic field mixes with axions*. Denoting the amplitude of this parallel photon component with A and the amplitude of the axion field with a , our linearized wave equation reads (Raffelt and Stodolsky 1988)

$$i\partial_z \begin{pmatrix} A \\ a \end{pmatrix} = \begin{pmatrix} n_\gamma\omega & B_t/2M \\ B_t/2M & \omega - m_a^2/2\omega \end{pmatrix} \begin{pmatrix} A \\ a \end{pmatrix} \quad (15)$$

with B_t the component of \mathbf{B} transverse to the wave vector \mathbf{k} , and M is defined by Eq. (4). The photon refractive index n_γ is, in general, complex because of absorptive effects in the medium.

b) An upper limit to the expected x-ray flux

Assuming, at first, that the diagonal entries of this matrix were real and equal, assuming a homogeneous field, and that the beam contains only an axion component at the beginning of the field region, one easily finds that after a distance ℓ the probability of measuring a photon is given as

$$p(a\rightarrow\gamma) = |B_t\ell/2M|^2. \quad (16)$$

This approximate result holds only if $p \ll 1$. For $B_t = 3$ Tesla and $M = 1\times 10^{10}$ GeV we find $B_t/2M = 1.48\times 10^{-12}$ cm $^{-1}$ so that for path-lengths in the meter range this condition is well-satisfied. This transition rate sets an absolute ceiling to what one can achieve with a given field strength and a given path length. All effects which occur from the non-equality of the diagonal entries in our mixing matrix reduce this

* By “parallel” component we mean the polarization state whose electric field vector lies in the plane of the wavevector \mathbf{k} and the magnetic field \mathbf{B} . It is parallel to \mathbf{B} only if the propagation is strictly transverse to the magnetic field.

result. Taking now $B_3 = B_t/3$ Tesla, $\ell_4 = \ell/4$ m, and again $M_{10} = M/10^{10}$ GeV, an absolute ceiling to the expected x-ray flux from solar axion conversion is thus

$$F_\gamma = 1.2 \times 10^{-7} \text{ cm}^{-2} \text{ sec}^{-1} B_3^2 \ell_4^2 / M_{10}^4 \quad (17)$$

where we have used the result Eq. (12). This result sets the scale for the x-ray fluxes we are concerned with. The x-ray spectrum would follow Eq. (14) with an appropriate normalization.

c) General result for the transition rate

In general, the dispersion relations for axions and photons are not identical. However, for x-rays in the keV range and for a low- Z gas as a medium, photons propagate approximately like massive particles. Thus we write for the photon refractive index

$$n_\gamma \omega = \omega - m_\gamma^2 / 2\omega - i\Gamma/2, \quad (18)$$

where m_γ may vary in space because of density gradients of the medium, and it also contains a weak residual dependence on ω . Γ is the damping coefficient, or inverse absorption length, for the x-rays so that the intensity of a beam decreases as $e^{-\Gamma z}$. The quantities m_γ and Γ are easily related to the usual atomic scattering factors f_1 and f_2 as tabulated, e.g., by Henke *et al.* (1982). In order to determine a general solution to the ‘‘Schrödinger equation’’ Eq. (15) we make use of the ‘‘perturbed wavefunction’’ approach outlined by Raffelt and Stodolsky (1988). Note, however, that the ‘‘Hamiltonian’’ in Eq. (15) is not Hermitian so that one has to modify the procedure to solve this equation accordingly. From a first order perturbative solution we then find for the transition *amplitude*, aside from an overall phase,

$$\begin{aligned} \langle A(z)|a(0) \rangle &= (1/2M) \exp\left\{-\int_0^z dz' \Gamma/2\right\} \times \\ &\times \int_0^z dz' B_t \exp\left\{i \int_0^{z'} dz'' \left[(m_\gamma^2 - m_a^2)/2\omega - i\Gamma/2\right]\right\}. \end{aligned} \quad (19)$$

This result is first order in the small quantity $B_t z/2M$, but completely general otherwise. Note that, in general, B_t , Γ , and m_γ are functions of z . If we now assume that all of these quantities are constant in space, and if we introduce the oscillation length by

$$2\pi/\ell_{\text{osc}} = |(m_\gamma^2 - m_a^2)/2\omega| \quad (20)$$

the transition rate is found to be, for a path length $z = \ell$,

$$p(a \rightarrow \gamma) = \frac{(B_t/2M)^2}{(2\pi/\ell_{\text{osc}})^2 + \Gamma^2/4} \left[1 + e^{-\Gamma\ell} - 2e^{-\Gamma\ell/2} \cos(2\pi\ell/\ell_{\text{osc}}) \right]. \quad (21)$$

In the absence of damping ($\Gamma = 0$) this is the usual result for the transition between two mixed particle states.

4. The detector

4.1 Basic concept

The heart of the detector would be the FNAL 15 foot bubble chamber magnet: coil and cryostat, refrigerator and helium inventory. Possibly we will also want the vacuum tank and the bubble chamber itself.

Since the Primakoff effect is an $\mathbf{E} \cdot \mathbf{B}$ interaction, it is important that the magnetic field be perpendicular to the line-of-sight to the sun to maximize the conversion probability. This implies that we will want to mount the axis of the Helmholtz pair at an angle $90^\circ - \Theta_{\text{latitude}}$, on the average at least, and if possible allow for the equinoctial variation of $\pm 23^\circ$.

Inside of the magnet bore is a vessel containing hydrogen or helium gas for matching of the axion and photon dispersion relations. The rear semicylindrical surface is instrumented with high-efficiency, low-noise detectors for x-rays in the (1 – 10) keV range. The area transverse to the Sun's line-of-sight for which the magnetic field is a meaningful fraction of the central value of 3 Tesla is about 15 m^2 . In order that the helioscope have pointing ability there will be a collimator structure, which could be an array of hexagonal close-packed tubes, with the x-ray detectors at the end of each tube. The array of tubes, while costing a small packing fraction factor, are the most attractive option. This is so because the tubes, rather than the tank itself, will serve the role of containing the gas whose pressure will be very great while searching in the higher mass region. Since the *density* determines the index of refraction rather than the *pressure*, we may obtain higher gas densities at lower pressures by cooling the gas. This will necessitate a double-walled cryostat. The tubes should have a diameter of perhaps 3" or so, in order that the aperture effect be negligible. The inner vessel at least will be free-standing from the magnet, as it will have to be gimballed and

continuously rotated to point at the Sun 24 hours a day. A cutaway isometric view of a possible design is shown in Fig. 4.

4.2 Counting rates

To calculate estimated counting rates for the experiment, we have made a simplified model for the detector. We assume that the clear bore of the magnet is 4 m in diameter, that its usable length is 3 m, and that the magnetic field is 3 T everywhere within this volume. We further assume for now that the entire rear semicylindrical surface is instrumented with x-ray detectors of unit efficiency, and we do not worry about lost area due to detector packing fraction, *etc.*, which would introduce a reduction factor of about 0.5.

The pressure required to match the effective mass for x-rays in the medium with the axion mass is found by expressing the real part of the photon dispersion relation by an effective mass in the spirit of Eq. (18),

$$m_\gamma^2 = 4\pi r_0 (N_A/A m_u) \rho f_1. \quad (22)$$

Here r_0 is the classical electron radius, N_A is Avogadro's number, A is the relevant atomic mass number, m_u the atomic mass unit, ρ is the gas density, and f_1 is the real part of the atomic scattering factor as tabulated, e.g., by Henke (1982). The use of the lowest- Z gas possible is clearly indicated on two counts. First, the real part of the atomic scattering factor f_1 is linear in Z , whereas the absorptive part (proportional to the mass attenuation coefficient) increases roughly as Z^3 . Second, the variation of $f_1(\omega)$ in the relevant range $\omega = (1 - 10)$ keV is sufficiently weak only for H_2 and He so that the matching of the dispersion relations can be achieved *simultaneously* over this entire range of frequencies. For these gases, the asymptotic value $f_1(\omega \rightarrow \infty) = Z$ is taken on with sufficient precision over our entire range of interest. Fig. 5 shows the pressure of either H_2 or He gas as a function of axion mass; note the m_a^2 dependence, as well as the absolute values required for the high-mass end of the scale if the gas is at room temperature. The advertised upper mass limit of our experiment is somewhat arbitrary and determined by the practical issues posed by gas handling at high pressures. The virtue of cooling the gas to liquid Ne temperatures is obvious—compare the right- and left-hand scales of Fig. 5.

For a given mass of the axion, the total conversion rate over the whole rear semicylindrical surface of the detector and over the whole axion spectrum is given by

$$R = H \int dy \int dE_a F'_a p_{a \rightarrow \gamma}[z(y)]. \quad (23)$$

Here H is the height and D the diameter of the cylinder instrumented with detectors, F'_a is the differential solar axion flux as given by Eq. (14), and $z(y) = 2\sqrt{(D/2)^2 - y^2}$ is the length of the chord through the cylinder at transverse position y . The conversion rate $p_{a \rightarrow \gamma}[z(y)]$ depends on the axion-photon coupling strength, and implicitly on both m_a and E_a through ℓ_{osc} as given by Eq. (20). We have incorporated the effect of photon attenuation by using $p_{a \rightarrow \gamma}$ as given by Eq. (21). The result is shown in Fig. 6 for the relationship Eq. (2) between m_a and the axion-photon coupling with the assumed GUT value $E/N = 8/3$. Aside from absorptive effects—most evident at large values of m_a and rendering H_2 preferable to He —the overall rate goes as m_a^4 . It is seen that for m_a in the eV range, the rate will be large, perhaps many per second. The nominal lower end of our experimental sensitivity in mass, $m_a \approx 0.1$ eV, corresponds to a rate on the order of 1 day^{-1} . While again somewhat arbitrary, this lower limit anticipates solutions to the challenge of background reduction to that level.

At a fixed pressure P_0 , the response of the detector will be a sharply peaked function of m_a . In Fig. 7 we show the integrated rate as a function of m_a , where the pressure has been optimized for $m_0 = 1.000$ eV. The full-width fifth-maximum here is seen to be $(\Delta m/m_0)_{1/5} \approx 0.0022$. Here, Δm is the difference between the actual axion mass m_a and the value m_0 at which the counting rate would be optimal, $\Delta m = |m_0 - m_a|$. It is easy to show that the width of the response curve scales as m_0^{-2} (see Fig. 8). As a rough rule of thumb the full-width half-maximum is approximately $(\Delta m/m_0)_{1/2} \approx 0.0012 (m_0/\text{eV})^{-2}$. This implies that the experiment will be a *tuning* search in pressure. Later we will comment briefly on the implications for the strategy of the search, the demands on the stability and uniformity of the gas density, and the running time of the experiment.

If axions were found to exist, the spectrum of x-rays measured in the detectors at the rear of the pressurized tube array would faithfully reproduce the axion spectrum (Fig. 2) aside from absorptive effects and assuming the pressure is optimized for the relevant axion mass. If the pressure were set substantially off the maximum of the response curve, the measured spectra and distribution in transverse position y would be modulated non-trivially as the oscillation length $\ell_{\text{osc}}(m_a, E_a, P_0)$ became comparable to $z(y)$.

4.3 Detection of x-rays

One of the principle efforts of this experiment will be the R&D of x-ray detectors for the (1 – 10) keV range which can be made cheaply over a large area, have unit efficiency, and extremely low background. We are just at the outset of this study. Unfortunately, the energy of the x-rays is just high enough that clever schemes to reflect and focus x-rays from the entire back semicylindrical surface onto a small Si(Li) detector using multilayer optics will not work (Barbee 1988). Thus it will be necessary to instrument the entire back surface of perhaps 15 m².

a) Large area silicon detectors

The most desirable alternative would be the use of large area Si(Li) detectors. The depletion depth would be chosen to provide reasonable efficiency for detecting few-keV x-rays, but minimize the Compton scattering of high energy γ -rays from background radioactivity. As the photoelectric cross section is strongly energy-dependent ($\propto E^{-7/2}$), the signal-to-noise ratio may be optimized by a judicious choice of depletion depth. A preliminary analysis roughly favors 10 μ .

If we opt for a hexagonal close-packed tube array, the Si(Li) detectors would be mounted inside and would only require a feedthrough at the back wall of the tube. As the tubes will be on the order of 3" diameter, this implies around 2500 such silicon detectors. The unit price for such a large detector normally is very high (around \$ 1000.00) in small orders. However, we have had informal discussions with a company in Southern California concerning our application, and it seems possible that in large quantity the price may fall by an order of magnitude. Of course, the contractual product specifications and factory diagnostics would be much more relaxed than those for small orders of devices for high-resolution spectroscopy. We are optimistic concerning this possibility.

b) Inorganic scintillators

The next most attractive concept would be the use of very thin crystals of an inorganic scintillator, e.g., CsI(Tl) in conjunction with one or more large area (1 cm²) PIN diodes. CsI for photon detection has been undergoing a renaissance in recent years, e.g., the CLEO II electromagnetic calorimeter will be fabricated of CsI(Tl). It has the highest photon yield of any known material, 52 photons/keV (Holl 1987), it is only mildly hygroscopic, unlike NaI(Tl), and it is easy to work with. Two features of CsI give room for optimism that the background rate may be kept low. First, a disk of CsI could be fabricated of the minimum thickness necessary to stop essentially

all of the x-rays, i.e., about 15 mg/cm^2 , which will also stop all of the resulting photoelectrons even at the highest energy of importance to us. This will minimize the Compton scattering, *etc.* from natural radioactivity. Second, the long decay time of the scintillation (about 900 ns at 300° K , and longer at very low temperatures) gives us pulse shape information. By digitizing the same signal both for a “long” and a “short” ADC gate, one should be able to discriminate against the prompt signals that would be due to either Cerenkov light in the optical coupling medium between the scintillator and the diode, or direct conversion in the diode itself. Large area PIN diodes (the Hamamatsu S 1790-02) can be cooled to reduce the dark current well below the signal level, and the unit cost will certainly be manageable (about \$ 30.00). The unfortunate aspect of this scheme is that the photon statistics in a non-ideal geometry would probably preclude any useful energy resolution: this would be an x-ray *counter* rather than a *spectrometer*.

c) Proportional chambers

The third avenue that will be explored, but about which we are least sanguine, is the use of Ar or Xe proportional chambers at the end of the pressurized tube array. Since x-rays will be readily absorbed by all but the thinnest films, it is clear that the pressure of the Ar or Xe proportional chamber will have to track the ballast gas (H_2 or He) precisely and reliably over three orders of magnitude in pressure range. Otherwise the window will be blown out or in. Furthermore, proportional mode operation will have to be demonstrated over the entire dynamic range displayed in Fig. 5, the last decade of which, we believe, is without precedent. Finally, the integrity of the window will have to be absolute: even the most minute amount of Ar or Xe leaking into the ballast gas for a particular tube would radically decalibrate the relationship between pressure and index of refraction, which ultimately is what must be controlled and monitored to within some fractional bandwidth in mass.

4.4 Engineering considerations

This section comprises a list of some of the more challenging technical aspects of the experiment concerning materials, design and construction, operation, monitoring, and others. Although we have not decided upon specific courses, we mention them to indicate that we are aware of the issues, have begun to address them seriously, and are optimistic about their solution.

a) Pressurized tubing array

In Fig. 5 we showed the operating pressure of either H₂ or He gas as a function of axion mass for two different temperatures, one at Standard Temperature (273° K), and the other at LNe (27° K). It is clear that at room temperature, the pressure for searching in the several eV range will be formidable, $P_0 \approx 4000$ psi at $m_a = 4$ eV. Chrome-nickel stainless steel piping for plant processing applications in the several-inch diameter range have a typical wall thickness-to-diameter ratio of about 0.14 for 4000 psi. As this scales roughly with pressure, one may estimate that the weight of the tube array alone would be roughly $8(m_{\text{max}}/\text{eV})^2$ tons, where m_{max} is the upper limit of the mass search. Thus for 5 eV as the upper limit of the experiment, the tube array would weigh about 200 tons! Additionally, stainless steel is notorious for the amount of radioactive contaminants it contains. This would probably be unacceptable in the present application.

An attractive option would be to cool the pressurized tube array to liquid nitrogen temperatures, and perhaps one could even contemplate liquid neon. This would have very significant beneficial effects. It would permit the use of much thinner walled material, because the pressure would be reduced by a factor of 4 (at 77° K), and because all materials increase considerably in allowable stress when cooled. Then a number of alternative “clean” materials (titanium or even synthetic composites) could be used.

b) Gimbaling

The requirement of pointing the helioscope at the Sun necessitates that the vessel containing the tube array and detectors be free-supported from the magnet, and rotate smoothly at 15° per hour. The materials and drive mechanism must be designed keeping in mind the strong unclamped magnetic field of the 15' bubble chamber magnet (0.25 kG at 5 m).

Since the conversion probability scales with B_t^2 , it is very important to be able to orient the axis of the coil at an angle with respect to vertical, and preferably that this angle be adjustable. The support of the coils in the cryostat was not designed to take up large shear forces—a problem that needs to be studied.

c) Vacuum tank and cold vessel for the detector

The detector will probably be designed for cryogenic operation, requiring a double-walled vessel. In Fig. 4 we show a possible scheme, with both walls within the clear bore of the magnet. Other options include the use of the existing vacuum tank and the bubble chamber itself in our design.

d) Temperature uniformity and monitoring

For the coherent conversion of axions into photons it is important that the gas density be equal along the length of each tube. Since the gas will be static, and all the tubes will communicate with one another through their respective feed lines from a manifold, the entire experiment is guaranteed to be isobaric. The pressure gradient due to gravity—the “law of atmospheres”—is negligible in the present case so that isodensity is equivalent to isothermality.

To a lesser degree it is desirable that the density of all tubes be the same. If this is not satisfied, the situation can be recovered so long as the thermistry permits accurate knowledge of the density (and thus index of refraction) of each tube. Assuming the existence of the axion in our range of sensitivity, as one scans different tubes would go through the conversion resonance at values of the pressure slightly displaced from one another. However, a significant density gradient along one single tube itself implies an averaging or smearing of its response curve. In practice, as the orientation of the tubes is at an arbitrary angle, it is difficult to imagine having each tube as an isotherm without having the entire array (of a few meters linear dimension) as an isotherm.

The mass bandwidth translates into a condition on the temperature uniformity according to $\Delta T/T = 2\Delta m/m_0$. Again, m_0 is the axion mass for which the detector response at a chosen pressure P_0 is optimal. If one does not wish to smear the response of any tube beyond the full-width half-maximum of the resonance, this implies $\Delta T/T < 0.002 (m_0/\text{eV})^{-2}$. For the smallest masses, where the expected counting rate is very low, the bandwidth in mass is largest. In fact, the bandwidth in mass is quite large at the lower mass limit of this experiment, about 0.1 at $m_0 = 1 \text{ eV}$. One might argue that the temperature uniformity condition is needlessly stringent at the higher mass (few eV) end: one could afford smearing over a much wider fraction of the mass as the absolute conversion rate would be expected to be acceptably large even far down on the tails of the resonance. Such an argument should be viewed with caution: the relation between m_a and the axion-photon coupling is not known *a priori* and indeed there are models where the axion-photon coupling may be highly suppressed ($E/N = 2$, Kaplan 1985). Strictly adhering to the condition that the response curve not be averaged beyond its FWHM implies a temperature uniformity of 6° mK at LN_2 , for $m_0 = 5 \text{ eV}$. This small value for the maximum allowable deviation from temperature uniformity and the requisite monitoring is potentially a problematic point with cryogenic operation.

We will examine how good an isotherm one can hope to achieve for the proposed geometry. The first obvious candidate would be a cryogenic bath with a gas-liquid

interface above the tops of the tubes. The other is a cooled minimum two-point support for the array inside a cryo/vacuum vessel. In addition to the radiative and possible conductive inward heat flow, we have to assess the importance of the heat source represented by the reverse current of thousands of silicon diodes.

4.5 Backgrounds

The ultimate limit to the sensitivity of the proposed search is set, on the low-mass end, by background. Background events can be generated by three sources, radioactivity in the materials of the detector and its environment, cosmic ray interactions, and detector noise. Radioactivity is by far the most serious background in a deep underground environment. The main background rate of the detector is then a product of three factors,

- The total rate R_γ of the photons traversing the detector elements due to radioactivity,
- the probability P_c that these photons scatter within a detector element, and
- the probability P_x that the signal produced is indistinguishable from a few-keV x-ray.

Measurements in the Gran Sasso laboratory indicate a photon background from the rock of $r_0 \approx 30$ Hz/kg. Of comparable importance may be the background from the magnet coil itself, which has not yet been measured, because it will also nearly surround the detector. Taking for now only the contribution from the surrounding rock, a rough approximation yields $R_\gamma \approx r_0 \lambda A/2 \approx 15$ kHz. Here, λ is the mean free path of a 500 keV γ -ray, $\lambda \approx 10$ g/cm², and $A/2 \approx 5$ m² is the average solid angle-area product subtended by the detector elements. By a careful choice of shielding and building materials (pre-war steel, virgin lead, etc.) we hope to reduce this locally to $R'_\gamma \approx 500$ Hz.

Regarding the probability for scattering in the detector elements, a Compton cross section of about 5 barns and a depletion depth of 10μ in a Si(Li) detector yield the *total* Compton probability of $P_c \approx 2.5 \times 10^{-4}$.

In order to estimate what fraction P_x of the scattered γ -rays ($E_\gamma \approx 500$ keV) will be indistinguishable from a low-energy x-ray ($E_x \approx 5$ keV), we assume that the Compton spectrum is flat. Thus $P_x \approx E_x/E_\gamma \approx 10^{-2}$.

However, we envision a geometry by which each detector element will be backed by about 2λ of active shielding, e.g., NaI with a photodiode, giving us an additional Compton suppression of $P_{\text{shield}} \approx 0.15$.

Taking all of these factors together, we find a total background counting rate of

$$R_{\text{background}} = R'_\gamma P_c P_x P_{\text{shield}} \approx 2 \times 10^{-4} \text{ Hz}. \quad (24)$$

This corresponds to a rate of roughly 16 day^{-1} . We note that at $m_a = 0.1 \text{ eV}$ the expected signal would be on the order of 1 day^{-1} . Given the roughness of our present estimates, it is clear that a much more careful study of the background rates is needed to establish the possibility of reaching, indeed, our advertised lower end of 0.1 eV .

4.6 Operational strategy

This experiment is a *tuning* experiment by which the ballast gas pressure P_0 is varied in order to enhance the conversion probability of the axion into an x-ray, over a narrow window in mass. A detailed *strategy* of how to allocate search time is premature as it depends critically on knowledge of backgrounds. Nevertheless, we can estimate the total number of discrete steps which the experiment will require, and the total time, assuming we wish to see 1 “true” event per mass “window”.

If the pressure P_0 is set such that the conversion rate is optimal for a mass m_0 , this rate is approximately

$$R(m_0) = 3 \times 10^{-2} \text{ sec}^{-1} (m_0/\text{eV})^4. \quad (25)$$

The fractional full width half maximum of the response curve as a function of the actual axion mass m_a is

$$F_{1/2}(m_0) = (\Delta m/m_0)_{1/2} \approx 10^{-3} (m_0/\text{eV})^{-2}. \quad (26)$$

Thus using only the FWHM of the response curve and ignoring its tails, the relevant number N_{steps} of discrete steps in gas pressure for a range (m_1, m_2) of axion masses is

$$N_{\text{steps}} = \int_{m_1}^{m_2} \frac{dm_0}{m_0 F_{1/2}(m_0)} \approx 500 (m_2^2 - m_1^2)/\text{eV}^2 \approx 500 (m_2/\text{eV})^2. \quad (27)$$

Similarly, the total measuring time t_{search} is given by

$$t_{\text{search}} = \int_{m_1}^{m_2} \frac{dm_0}{m_0 F_{1/2}(m_0) R(m_0)} \approx 1.6 \times 10^4 (m_1^{-2} - m_2^{-2}) \approx 1.6 \times 10^4 (m_1/\text{eV})^{-2}. \quad (28)$$

Thus the total search time would be $t_{\text{search}} \approx 20$ days if one attempts to reach to an axion mass of 0.1 eV. This, of course, ignores “off-times” when the magnetic field is off, or the helioscope is pointed away from the Sun, etc., interleaved with the “on-times” so as to continuously monitor backgrounds.

If a candidate axion signal were detected, the detector would be operated at the appropriate mass setting for an extended period of time to improve the signal-to-background ratio, perform a time correlation analysis, and so on. Should the axion then be found to exist, its mass would be determined with extreme accuracy.

5. Proposed initial work and milestones

It is clear that considerable engineering and R&D needs to be performed before the experiment can actually be mounted. Nevertheless we believe that the scientific case for this experiment is firm, both in terms of its niche in the overall axion picture, and in terms of its methodological soundness. Thus we have decided to submit at this PAC to avoid loss of a whole year. We propose to proceed by the following initial plan of work and milestones for the next six months.

5.1 Initial work on the part of FNAL

We request that no permanent disposition of the 15' bubble chamber (magnet, refrigerator, vessels, gaseous inventories, *etc.*) be made until we are able to present a more detailed plan no later than fall of this year. Moreover, we request that a FNAL engineer and designer be committed to develop a plan with us for the disassembly, moving, and setting up of the magnet and ancillary equipment.

5.2 Initial work on our part

We commit ourselves to meet the following goals by the fall of this year.

a) Detector concept and prototype

Decision on the concept as early as possible, and demonstration of a successful prototype x-ray detector for these conditions and geometry.

b) Backgrounds

Over the next several months we will perform a characterization all relevant gamma activities from the existing bubble chamber magnet, proposed construction materials (by sample procurement), and the site environment when determined. The impact of these activities on the actual detectors must be better understood and the lower mass limit of the experiment more clearly determined.

c) Preliminary design

Reasonably final solutions to the issues discussed in Sect. 4.4 can be expected, along with a preliminary design. Particular emphasis must be given to the question of temperature (and thus density) uniformity, and how the detector and tube array will be cooled.

d) Hazards

A preliminary plan will be drafted for addressing the potential hazards associated with various gaseous inventories in areas of confined occupancy.

e) Siting

Possible sites for the experiment both in the U.S. and in Europe will be studied. Backgrounds will be the driving consideration.

f) Collaborators

The collaboration must expand in view of the work to be done. While we expect that more people will be added at the institutions already represented (students and postdoctoral researchers), there is need for another strong group. Fermilab personnel have played a vigorous role in axion searches for the past several years: Rochester-Brookhaven-FNAL microwave cavity dark matter search, BNL E-840 (approved), E-605, E-613 reanalysis, SLAC E-141, and extant FNAL proposal in search of the

GSI 1.8 MeV state in e^+e^- . We would be delighted to have Fermilab collaborators with us and play a strong role in this experiment.

g) Resources

A proposal is in preparation for submission to DOE for funding of the R&D required to evaluate this experiment. Initially this would cover the detector development, engineering studies, and on-site background measurements.

6. Personnel

A preliminary breakdown of the work described in Sect. 6 by institution is described.

a) Lawrence Livermore National Laboratory

LLNL will take responsibility for the engineering of the detector vessel, particularly its cryogenic and solar tracking aspects.

b) University of California at Berkeley

Georg Raffelt has made numerous contributions to the understanding of the astrophysical axion limits, including work on white dwarf cooling, detailed stellar evolution calculations, and bounds from the supernova 1987a. More important for our experiment is his definitive work on the role of plasma effects in stars, which significantly weakened the original bounds on hadronic axions, and which allows for a reliable calculation of the solar axion spectrum from the axion-photon interaction. Also, with L. Stodolsky he has developed the elegant axion-photon mixing formalism and has generalized it to include the effects of photon absorption.

c) Lawrence Berkeley Laboratory

Dennis Moltz has made his career measuring extremely rare and very low-energy nuclear decay modes in hostile environments. He brings considerable experience in background processes, and will be responsible for materials evaluation using LBL's facility for ultra-low γ -counting. While at ORNL, he played precisely this role in an axion experiment which was one of the final blows to the "standard" axion of Weinberg (1978) and Wilczek (1978).

d) Texas Accelerator Center

Russ Huson played a major role in the construction of the 15' bubble chamber magnet and will work with the designated FNAL personnel in scoping the moving and reconfiguration of the magnet.

e) Texas A&M University

The work towards a prototype x-ray detector will be managed by Peter McIntyre. Of the present collaboration he alone has experience in deep-underground physics, having performed a large-volume scintillator monopole search in a salt mine.

f) Ohio State University

Richard Boyd is nearing completion of a novel and competitive neutrino mass experiment, and also performs low-counting rate measurements of astrophysically interesting reactions induced by beams of unstable nuclei. He will be invaluable in understanding and reducing the influence of radioactive backgrounds on our large area detector array.

g) CERN

Harry Nelson (with Karl van Bibber) has published a recent calculation on the limits of invisible axions that could be set in a purely terrestrial experiment using the Primakoff coupling. He will be responsible for environmental background measurements at the candidate European sites.

REFERENCES

- Abbott, L., and Sikivie, P. 1983, *Phys. Lett.*, **120 B**, 133.
- Bahcall, J., *et al.* 1982, *Rev. Mod. Phys.*, **54**, 767.
- Barbee, T. W., Jr. 1988, private communication.
- Bellotti, E. 1988, *Nucl. Instr. Meth. A* **264**, 1.
- Cheng, H.-Y., 1987, Report IUHET-125, submitted to *Phys. Rep.*
- Davier, M. 1987, Report LAL 87-27, to be published.
- DePanfilis, S., *et al.* 1987, *Phys. Rev. Lett.*, **59**, 839.
- Dearborn, D. S. P., Schramm, D. N., and Steigman, G. 1986, *Phys. Rev. Lett.*, **56**, 26.
- Dine M., and Fischler, W. 1983, *Phys. Lett.*, **120 B**, 137.
- Iwamoto, N. 1984, *Phys. Rev. Lett.*, **53**, 1198.
- Henke, B. L., *et al.* 1982, *Atomic Data and Nuclear Data Tables* **27**, 1.
- Holl, I., Lorenz, E., Mageras G. 1987, Report MPI-PAE/Exp. E1.185, presented at the IEEE Nuclear Science Symposium, San Francisco, Oct. 21-23, 1987, and to be published in the IEEE Transactions on Nuclear Science.
- Kaplan, D. B. 1985, *Nucl. Phys.*, **B 260**, 215.
- Kephart, T., and Weiler, T. 1987, *Phys. Rev. Lett.*, **58**, 171.
- Kim, J. E. 1987, *Phys. Rep.*, **150**, 1.
- Maiani, L., Petronzio, R., and Zavattini, E. 1986, *Phys. Lett.*, **175 B**, 359.
- Mayle, R., *et al.* 1988, submitted to *Phys. Lett. B*.
- Melissinos, A. C., *etal* 1987, Experimental Proposal (approved Brookhaven Experiment E-840).
- Peccei, R. D., and Quinn, H. 1977a, *Phys. Rev. Lett.*, **38**, 1440.
- Peccei, R. D., and Quinn, H. 1977b, *Phys. Rev. D*, **16**, 1791.
- Preskill, J., Wise, M., and Wilczek, F. 1983, *Phys. Lett.*, **120 B**, 127.
- Raffelt, G. 1986, *Phys. Lett.*, **166 B**, 402.
- Raffelt, G. 1988, *Phys. Rev. D*, to be published.
- Raffelt, G., and Dearborn, D. 1987, *Phys. Rev. D*, **36**, 2211.
- Raffelt, G., and Seckel, D. 1988, submitted to *Phys. Rev. Lett.*
- Raffelt, G., and Stodolsky, L. 1988, *Phys. Rev. D*, in press.
- Sikivie, P. 1983, *Phys. Rev. Lett.*, **51**, 1415 (E) *ibid.* **52**, 695 (1984).

Srednicki, M. 1985, *Nucl. Phys.*, **B 260**, 689.

Tsuruta, S., and Nomoto, K. 1986, IAU-Symposium No. 24, *Observational Cosmology*, in press.

Turner, M. 1987, *Phys. Rev. Lett.*, **59**, 2489.

Turner, M. 1988, submitted to *Phys. Rev. Lett.*

Weinberg, S. 1978, *Phys. Rev. Lett.*, **40**, 223.

Wilczek, F. 1978, *Phys. Rev. Lett.*, **40**, 279.

FIGURE CAPTIONS

Figure 1

Feynman diagram for the Primakoff production of axions by the interaction of a photon with an electron or nucleus (top), and (bottom) axion-photon conversion in the electric or magnetic field of an external source denoted by a cross (\times).

Figure 2

Differential solar axion flux at the earth. We assume that axions are only produced by the Primakoff conversion of blackbody photons in the solar interior (“hadronic axions”), and we assume a standard solar model (Bahcall *et al.* 1982). The axion-photon coupling strength M is defined in Eq. (4). The solid line arises from a numerical integration over the Sun, the dashed line is an analytical approximation to this result as given in Eq. (14).

Figure 3

Radial distribution of the axion energy loss rate L_a of the Sun, normalized to unity if integrated over the entire sun. The radial coordinate r is in units of the solar radius R_\odot .

Figure 4

A cutaway isometric view of the detector.

Figure 5

Pressure of H_2 or He gas to optimize the detection of axions of a given mass. Left-hand vertical axis for $T = 273^\circ$ K, right-hand for $T = 27^\circ$ K (liquid Ne).

Figure 6

Total rate of axion-photon conversion as a function of the axion mass m_a , using Eq. (5) for the relationship between m_a and the axion-photon coupling M and assuming the GUT value $E/N = 8/3$. The pressure is assumed to be optimized for each value of m_a . At the largest m_a values, corresponding to large gas densities, the rate for He (dashed line) is less than that for H_2 (solid line) because of the increased importance of absorption for a higher- Z medium.

Figure 7

Integrated rate as a function of m_a if the gas pressure P_0 has been set to optimize the counting rate for axions of mass $m_0 = 1 \text{ eV}$. The dashed line is a blow-up of the solid line and corresponds to the scale on the upper horizontal axis.

Figure 8

The full-width fifth-maximum “bandwidth” in mass, $(\Delta m_a/m_0)_{1/5}$, as a function of the mass m_0 for which the pressure is optimized.

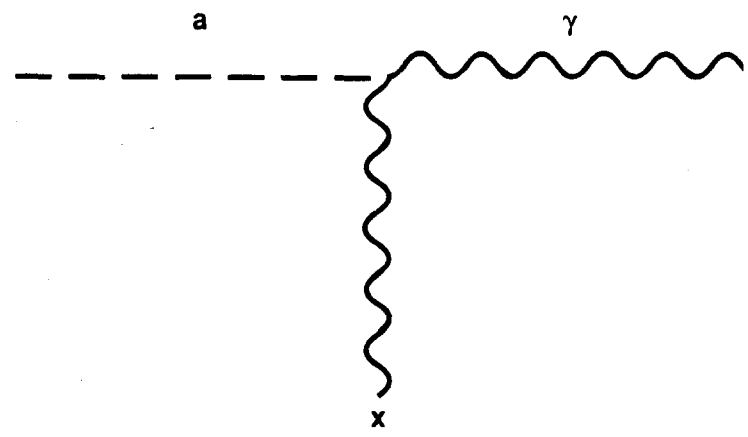
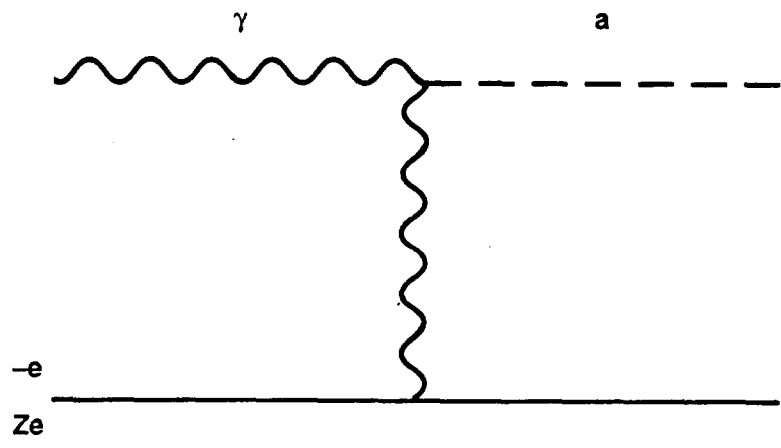


Figure 1

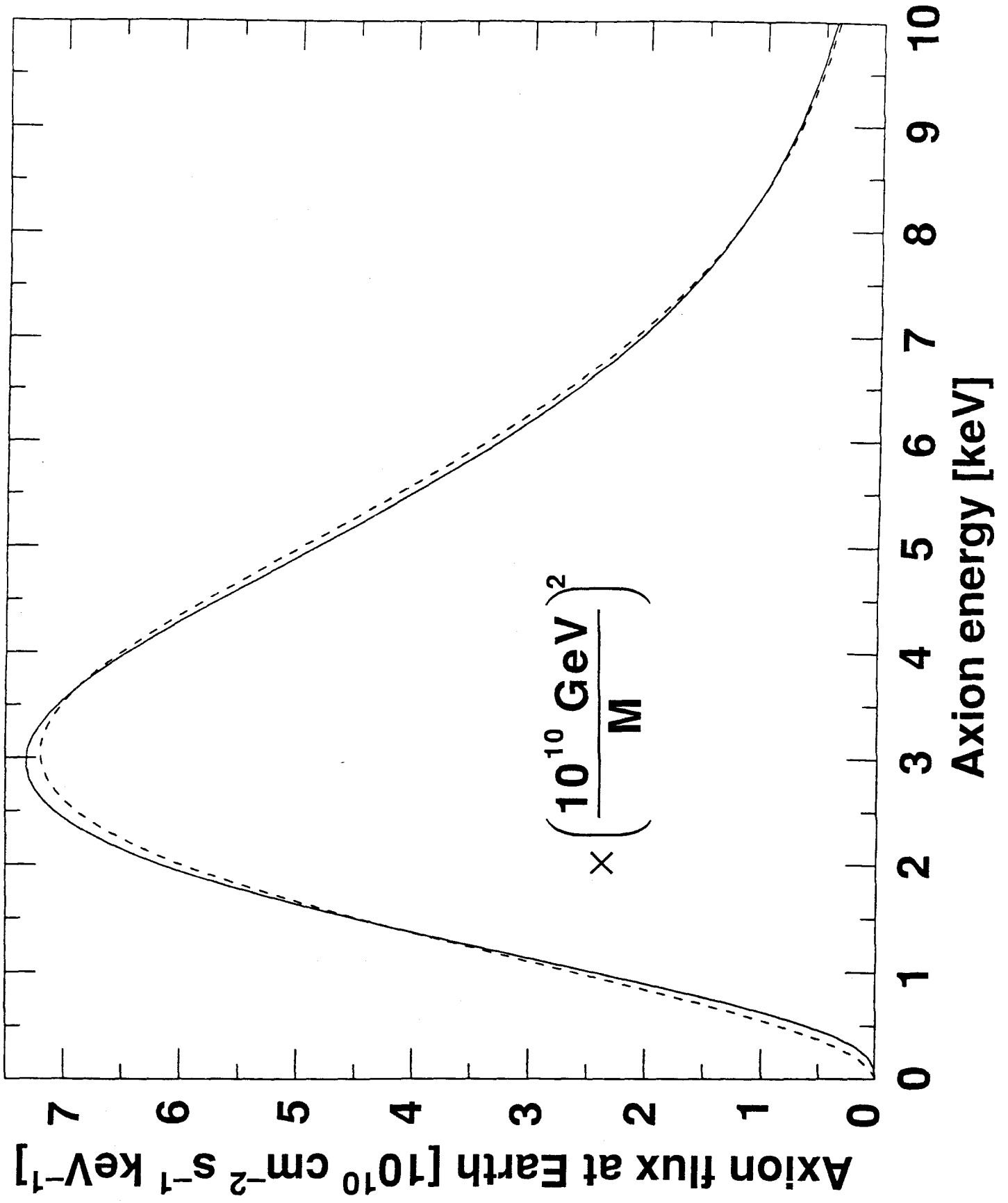


Figure 2

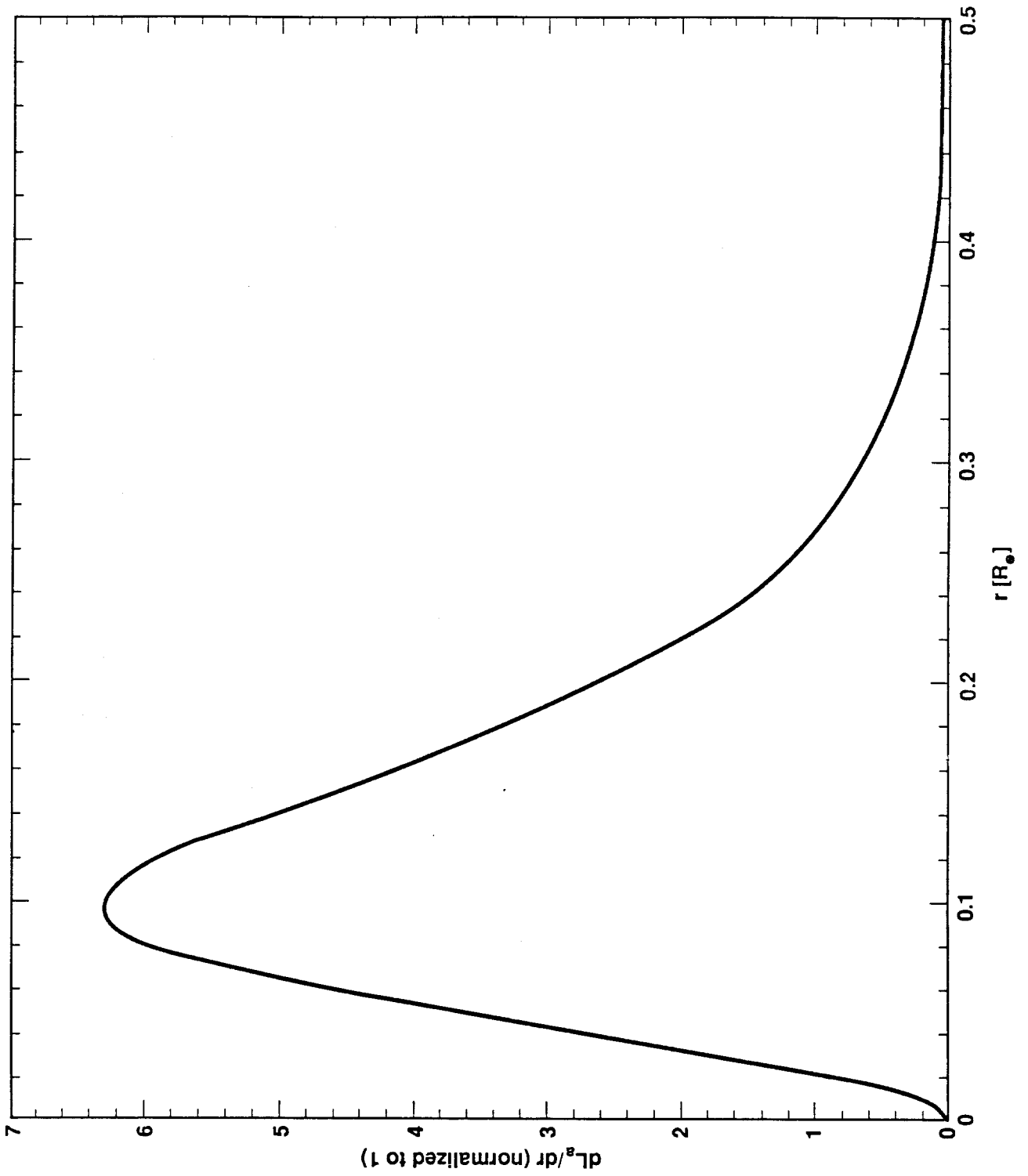


Figure 3

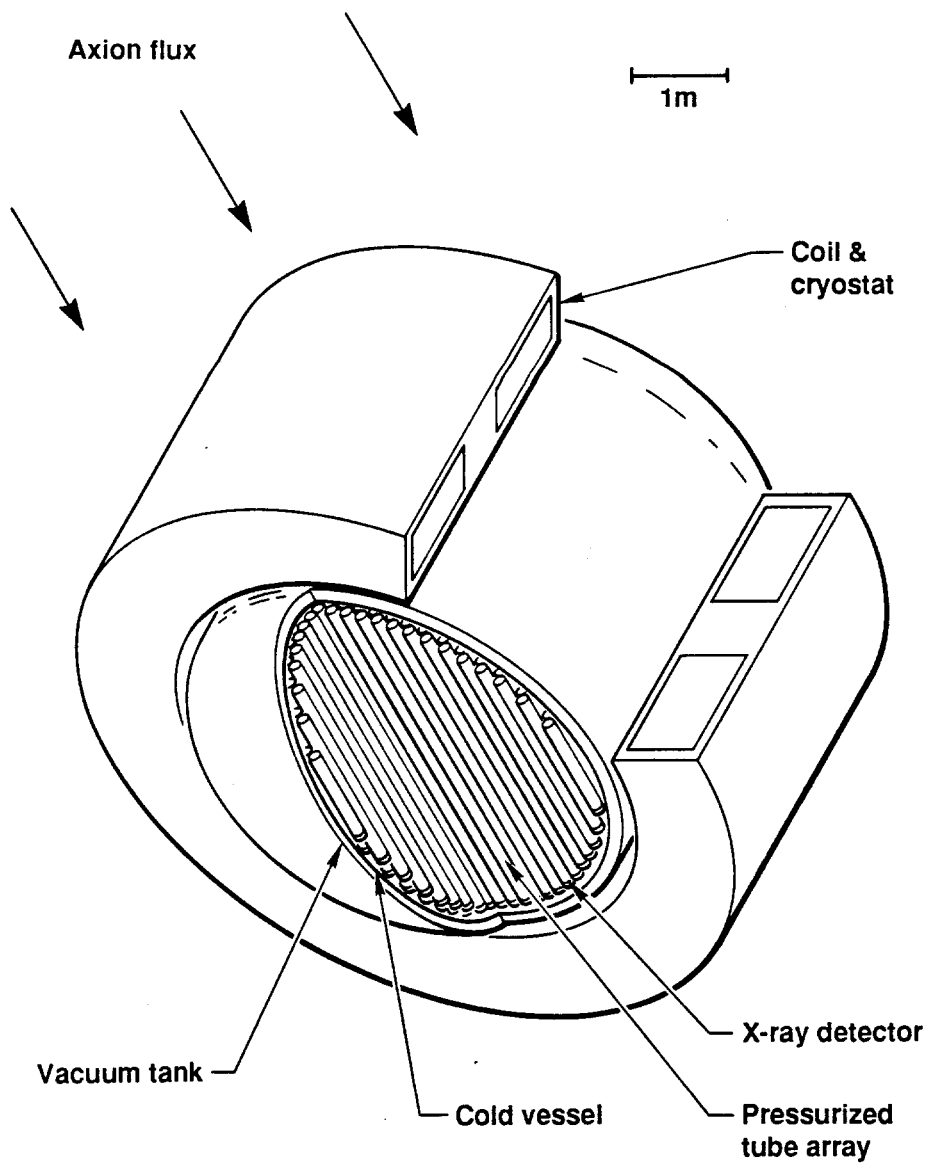


Figure 4

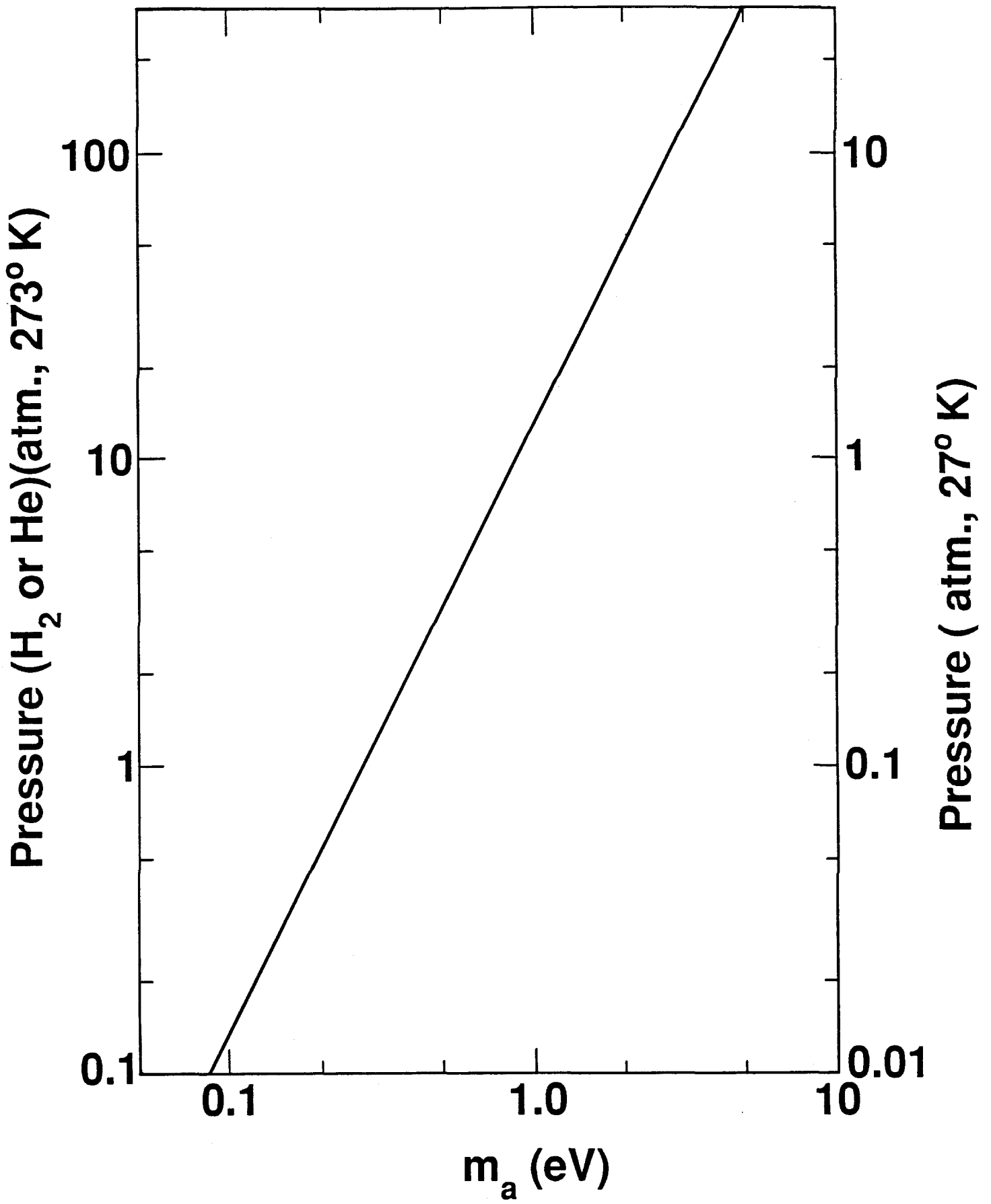


Figure 5

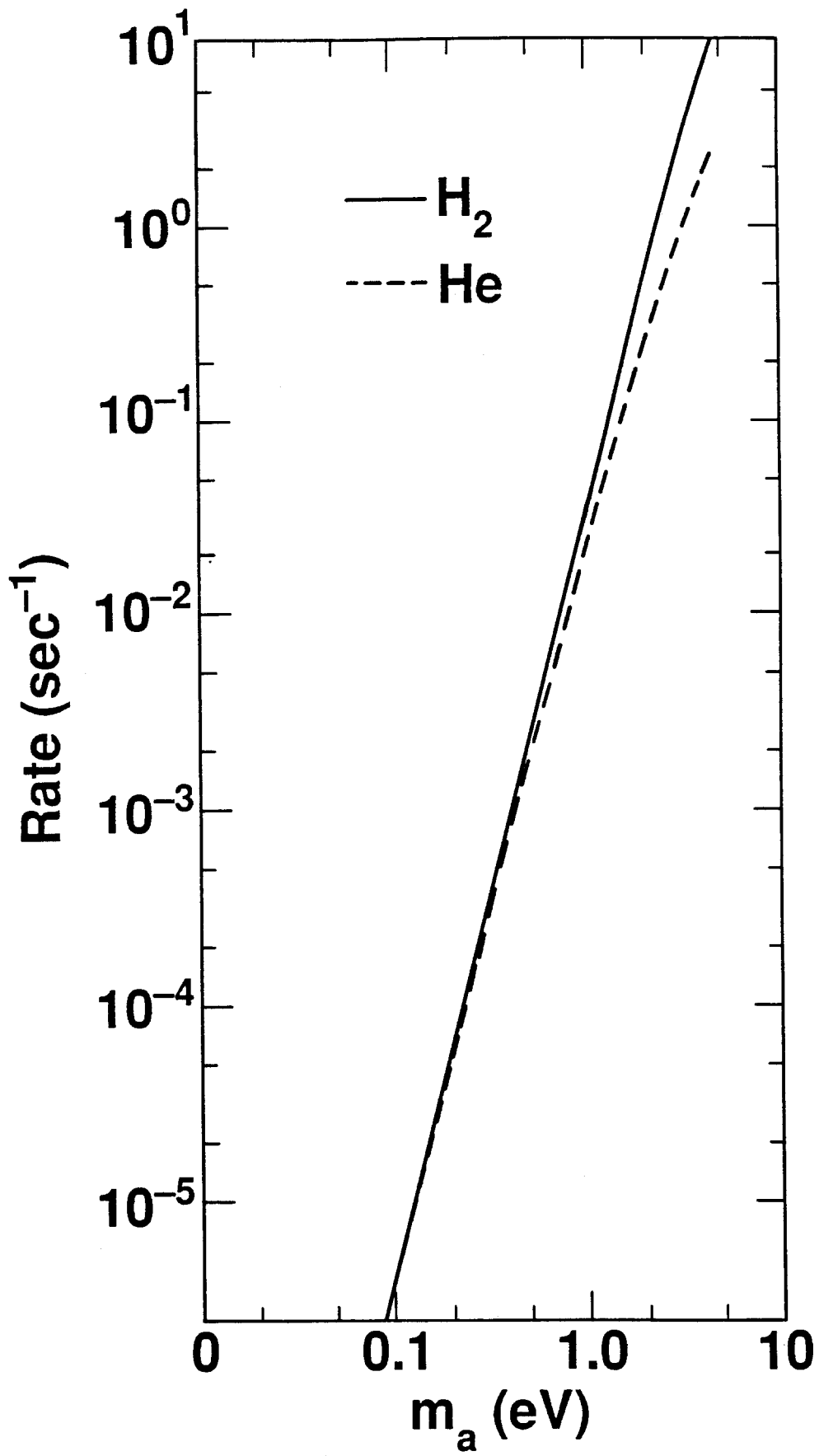


Figure 6

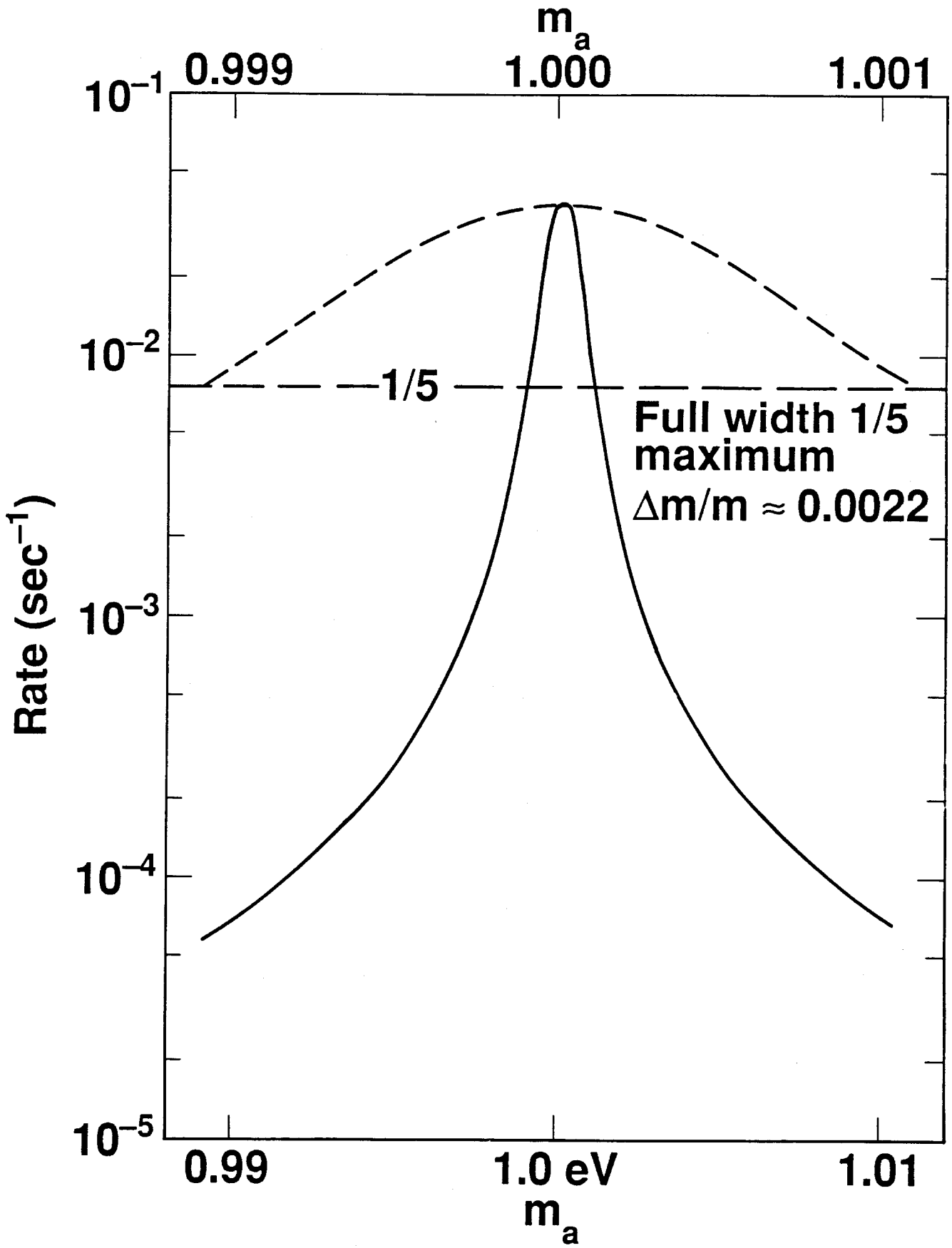


Figure 7

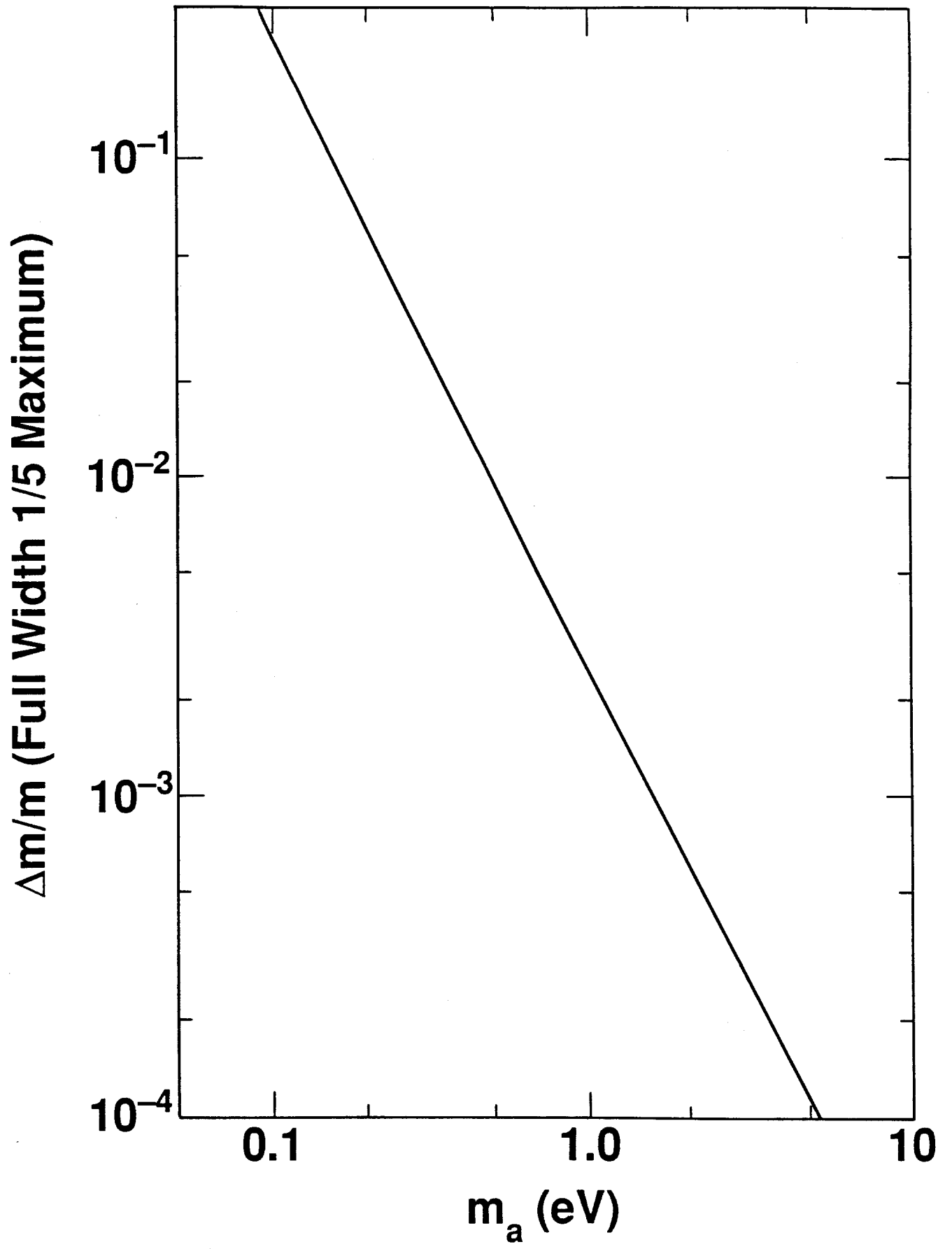


Figure 8